

Università Politecnica delle Marche  
Facoltà di Ingegneria  
Corso di Laurea in Ingegneria Informatica e dell'Automazione



# Lie-Group modelling and numerical simulation of a helicopter

Modellazione e simulazione numerica di un  
elicottero basate sui gruppi di Lie

Relatore:

Chiar.mo Prof. Simone Fiori

Candidato:

Alessandro Tarsi

Sessione Straordinaria

Anno Accademico 2019/2020

# Lie-Group modelling and numerical simulation of a helicopter

Alessandro Tarsi

## Abstract

This document introduces a mathematical model of a helicopter following the principle of Lagrange-d'Alembert-Pontryagin, tailored to Lie group  $SO(3)$ . The resulting system of equations is explained and enhanced with applications and numerical simulations in order to go into depth on the study of the model and typical behaviours of a helicopter. The implementation is provided by the software MATLAB, while the numerical resolution of the equations is performed by the forward Euler method (fEul). The fEul is consistently written taking into account that some equations belong to the rotational group  $SO(3)$ .

Supervisor: Chiar.mo Prof. Simone Fiori  
**Univerisitá Politecnica delle Marche**

# Modellazione e simulazione numerica di un elicottero basate sui gruppi di Lie

Alessandro Tarsi

## Sommario

Questo documento introduce il modello matematico di un elicottero seguendo il principio di Lagrange-d'Alembert-Pontryagin, particolarizzato per il gruppo di Lie  $SO(3)$ . Il sistema di equazioni risultante viene illustrato e arricchito di applicazioni e simulazioni numeriche in modo da scendere in profondità nello studio del modello e dei tipici comportamenti di un elicottero. L'implementazione si basa sul software MATLAB, mentre la risoluzione numerica delle equazioni sfrutta il metodo di Eulero in avanti (fEul). Quest'ultimo è stato scritto tenendo in considerazione che alcune equazioni appartengono al gruppo delle matrici ortogonali speciali  $SO(3)$ .

---

# Contents

|  |           |
|--|-----------|
| <b>List of Figures</b>   | <b>iv</b> |
| <b>List of Tables</b>  | <b>v</b>  |
| <b>1 Introduction</b>  | <b>1</b>  |
| <b>2 The Lagrange-d'Alembert-Pontryagin principle and the forced Euler-Poincaré equation</b> | <b>6</b>  |
| 2.1 Definition and properties . . . . .  | 6         |
| 2.2 The Euler-Poincaré equations . . . . .   | 7         |
| 2.3 Exemplary case: Euclidean space . . . . .  | 9         |
| <b>3 Mathematical model of a helicopter</b>  | <b>10</b> |
| 3.1 Model of a helicopter with a single principal rotor and a tail rotor . . . . .           | 11        |
| 3.2 Lagrangian function associated to the helicopter model . . . . .                         | 16        |
| 3.3 Rotational component of motion . . . . .   | 20        |
| 3.4 Translational component of motion . . . . .  | 21        |
| 3.5 Explicit state-space form of the equations of motion . . . . .                           | 22        |
| <b>4 Numerical aspects</b>   | <b>25</b> |
| <b>5 Helicopter type and value of the parameters</b>   | <b>27</b> |
| 5.1 Main rotor and tail rotor characteristics . . . . .                                      | 27        |
| 5.2 Dimensions and center of mass . . . . .  | 28        |
| 5.3 Engines and gear box . . . . .   | 30        |
| 5.4 Main rotor thrust and tail rotor thrust . . . . .  | 30        |
| 5.5 Drag term and friction terms . . . . .   | 31        |
| <b>6 Numerical experiments and results</b>   | <b>34</b> |
| <b>7 Conclusions</b>   | <b>42</b> |
| <b>Bibliography</b>  | <b>44</b> |

---

# List of Figures

|     |  |    |
|-----|--|----|
| 1.1 | Eurocopter EC 135, with a fantail assembly tail rotor (reproduced from <a href="https://en.wikipedia.org/wiki/Tail_rotor">https://en.wikipedia.org/wiki/Tail_rotor</a> ). . . . .  | 1  |
| 1.2 | <i>Collective control</i> changes the angle of attack of all blades at the same time. . .  | 2  |
| 1.3 | <i>Cyclic control</i> series of blade rotating frame. . . . .  | 3  |
| 1.4 | Anti-torque effect of the tail rotor. . . . .  | 3  |
| 1.5 | Illustration of the functioning of a swash-plate (taken from [1] page 272) . . .   | 4  |
| 1.6 | Illustration of the functioning of the pitch change spider (taken from [1], page 272) . . . . .  | 4  |
|     |  |    |
| 3.1 | Schematic of a helicopter with a principal rotor and a tail rotor (adapted from [2]). (The principal rotor to centre of mass distance $D_m$ and the tail rotor to centre of mass distance $D_t$ are expressed in meters (m)). . . . .        | 12 |
| 3.2 | Variation of the angle of attack along $x$ axis. . . . .   | 13 |
| 3.3 | Variation of the angle of attack along the $y$ -axis. . . . .  | 13 |
|     |  |    |
| 5.1 | Dimensions of the EC135 P2+, the picture is taken from [3]. . . . .  | 28 |
| 5.2 | Values used to calculate the centre of mass. Picture taken from [3], page 7. . .   | 29 |
| 5.3 | Friction terms increasing horizontal speed. The variables are defined as $F_z^1 = e_z^\top \varphi$ , $F_z^2 = M_H \bar{g}$ , $F_z^3 = e_z^\top \dot{p} \beta_v$ , $F_x^1 = e_x^\top \varphi$ , $F_x^2 = e_x^\top \dot{p} \beta_h$ . . . . . | 32 |
|     |  |    |
| 6.1 | Graphic input interface. . . . .   | 34 |
| 6.2 | First test - lift response. Top panel: components of the position of $c_H$ . Middle panel: components of the thrust. Bottom panel: components of the active torque generated by rotors. . . . .  | 38 |
| 6.3 | Second test - no yaw. . . . .  | 38 |
| 6.4 | Third test - neither yaw nor drift. . . . .  | 39 |
| 6.5 | Fourth test - pitch response. . . . .  | 39 |
| 6.6 | Fifth test - positive roll response. . . . .   | 40 |
| 6.7 | Sixth test - Main rotor collective response. . . . .   | 40 |
| 6.8 | Seventh test - negative roll response. . . . .   | 41 |
| 6.9 | Eighth test - free flight. . . . .   | 41 |

---

---

## List of Tables

|     |   |    |
|-----|---|----|
| 5.1 | Tail rotor collective angle range, tail rotor weight, speed main rotor ([1] page 303, 254 and 157), tail rotor speed ([4] page 3), cycling angle page (11 in [5]).  | 27 |
| 5.2 | Dimensions are taken from [3], page 7, and the weight of the main rotor blade from [6], page 3. . . . .   | 28 |
| 5.3 | Values are taken from [7], page 8 and 12. The helicopter state AEO means all engine operatives, whereas the state OEI is the short for one engine inoperative. Usually, the second state occurs when there is a problem in one engine. Typically, two possible working mode could be selected TOP (take-off power), which has a time limit constrain, and MCP (maximum continuous power). . . | 30 |
| 5.4 | Airspeed value ([8] page 23). Hover turning velocity and throttle range (page 43 and 35 in [3]). Rate of climbing (page 60 in [9]). . . . .   | 32 |
| 6.1 | Eighth test - free flight. The orange-colored numbers indicate that the <i>no-yaw</i> flight mode has been activated for that time window. . . . .  | 37 |

---

## Introduction

Conventional helicopters are built with two rotors. These can be arranged as two coplanar rotors both providing upward thrust, but spinning in opposite directions in order to balance the torques exerted upon the body of the helicopter. The two rotors can also be arranged with one main rotor providing thrust and a smaller side rotor oriented laterally and counteracting the torque produced by the main rotor, as shown in the Figure 1.1. Helicopters with no tail rotors ('notar') use a jet of compressed air to compensate for the unwanted yawing of the fuselage.



Figure 1.1: Eurocopter EC 135, with a fantail assembly tail rotor (reproduced from [https://en.wikipedia.org/wiki/Tail\\_rotor](https://en.wikipedia.org/wiki/Tail_rotor)).

Controls on a helicopter are numerous. Considering a rigid rotor system, the attitude and the position of a helicopter are mainly controlled through two systems, called *collective control* system and *cyclic control* system. The power exerted by the rotors is usually pretty constant, in fact, the blades are designed to operate at a specific rotational speed. However, it is possible to change the engine power slightly using the *throttle control*, whereas the direction the aircraft nose points, the yaw angle, could be changed using the *pedals control*. A summary of helicopter controls is given in the following.

***Collective control:*** The *collective control* is used to increase or decrease the total thrust generated by the rotors. This technique is adopted in the main rotor and in the tail rotor. To grow (to reduce) the thrust it is necessary to increase (to decrease) the angle of attack

of the all blades  $\alpha_c$ . This angle is in each instant equal for all the blades. An example of the usage of the *collective control* is illustrated in Figure 1.2.

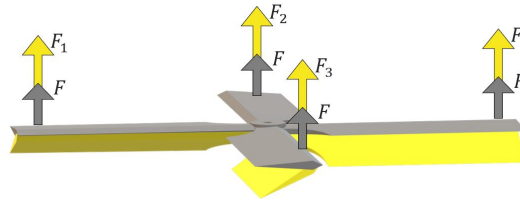


Figure 1.2: *Collective control* changes the angle of attack of all blades at the same time.

***Cyclic control:*** The *cyclic control* is distinctive of the main rotor. To tilt the body of a helicopter forward and backwards (pitch) or sideways (roll), the control must alter the angle of attack of the main rotor blades cyclically during rotation. As illustrated in Figure 1.3. In particular, controlling the angle of attack of the blades in such a way that the forward-hand half of the rotor disk exerts more (less) thrust than the backward-hand half makes the helicopter roll to the left (right). This effect is known as the conservation of angular momentum: a change of the angular momentum will create a torque in the direction described by the right-hand law. Generally, to change the attitude of a helicopter it is necessary to modify the angle of the thrust exerted by the main rotor, but the thrust is generated by the rotation of the blades, so it is necessary to create different amounts of thrust at different points in the cycle. Where a greater (smaller) amount of thrust is necessary the blade increases (decrease) its angle. The angles taken by the blades will be a function of time, the two angles  $\alpha_p$  and  $\alpha_r$  are used to indicate the angle of the thrust vector.

***Pedals control:*** Because of momentum conservation, the rotation of the main rotor causes a rotation of the body of the helicopter in the opposite direction: as the engine turns the main rotor system in a counterclockwise direction, the helicopter fuselage turns clockwise. The amount of torque is directly related to the amount of engine power being used to turn the main rotor system. The unwanted yawing of the fuselage may be balanced by controlling the thrust of the tail rotor, as illustrated in Figure 1.4. The anti-torque pedals change the tail rotor collective angle of attack  $\alpha_c^T$ . The yaw angle variation depends upon variations of the tail rotor thrust or variations on the main rotor thrust. The *pedals control* is used for heading changes while hovering, but also to maintain the actual helicopter nose direction.

***Actuators:***

- The *cyclic control* and the *collective control* of the main rotor work through a complex mechanical system called ‘swash-plate’, whose functioning is illustrated in Figure 1.5. The swash-plate is composed of two parts, one that is tight with the rotor mast and one that can rotate with the main rotor. Each blade is strictly connected with the swash-plate revolving part using a rod, this causes a variation of the angle of attack



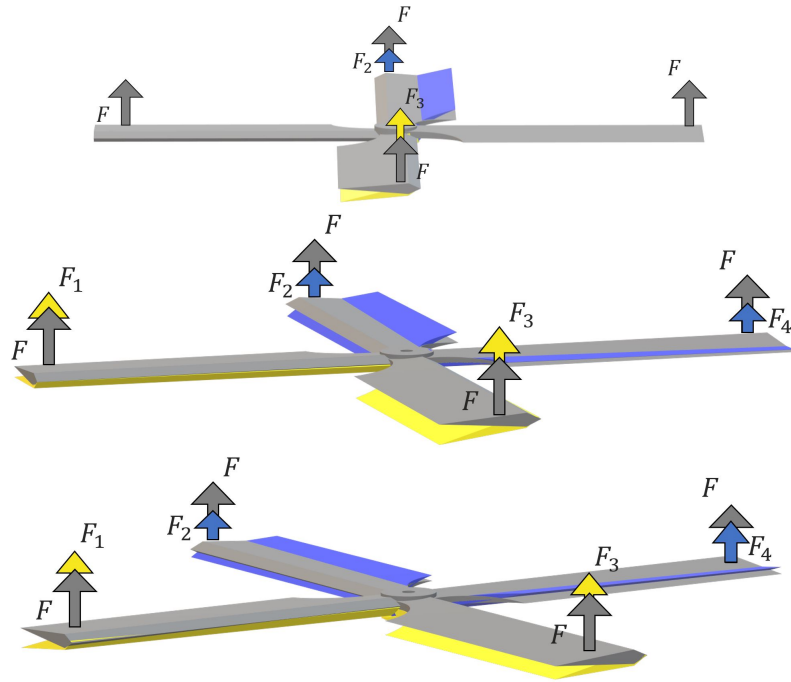


Figure 1.3: *Cyclic control series of blade rotating frame.*

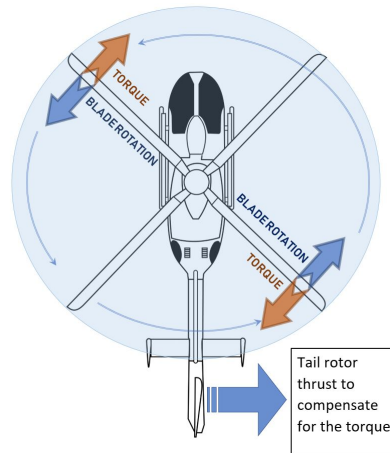


Figure 1.4: Anti-torque effect of the tail rotor.

of the blade when the swash-plate changes position. The swash-plate manages the cyclic and collective angles and sets up constraints in their ranges.

The *collective control* causes a movement upward or downward of the swash-plate on the rotor mast, therefore all the blades increase or decrease their angle simultaneously. The *cyclic control* changes the attitude of the swash-plate. This causes a changing of the angle of attack that is different in every part of the rotation cycle.

- The tail rotor collective angle  $\alpha_c^T$  actuator is called “pitch change spider” and, as like as the swash-plate, is used to change all the blades angle of attack simultaneously.

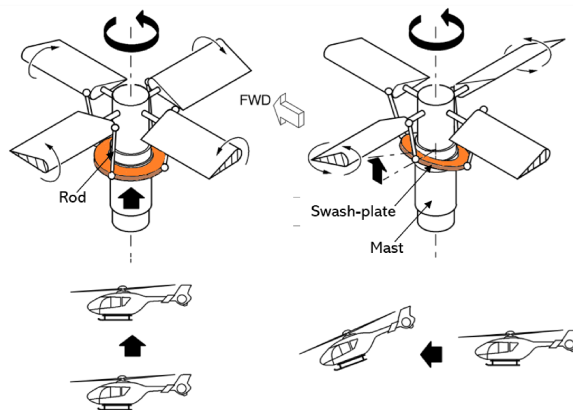


Figure 1.5: Illustration of the functioning of a swash-plate (taken from [1] page 272)

The Figure 1.6 explains how this works. Helicopters, usually, possess a stabilizer system that reduces the noise of the wind and manages the variations of the drag effect, providing an easier use of the yaw pedals. The pitch change spider sets up also the constrains for the range of variation of  $\alpha_c^T$ .

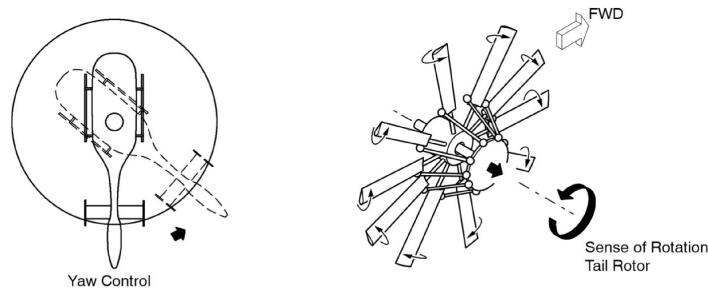


Figure 1.6: Illustration of the functioning of the pitch change spider (taken from [1], page 272)

**Throttle:** The throttle controls the power of the engine which is connected to both rotors by the transmission. The throttle setting must maintain enough engine power to keep the rotor speed within the limits where the rotor produces enough lift for flight. The value of the throttle changes the blades' angular velocity in a range of few values percentage. The helicopters have only a gear to drive both the main rotor and tail rotor, hence increasing the speed of the main rotor causes an increase of the tail rotor speed. More throttle means more speed and hence a larger value of thrust. The angular velocity of the rotors is usually reported in percentage for a more intuitive perception, the value of 100% is the typical one in standard condition.

In the present paper, we derive, through the Euler-Poincaré formalism, the mathematical

equations of a simplified helicopter model. The model concerns a helicopter with a principal rotor and a tail rotor. More accurate (and mathematically complicated) aircraft models are available in the specialized literature [10, 11, 12]. The structure of the paper is the following:

- *Chapter 2* presents a summary of definitions and properties regarding the Lie group, such as the tools used in this research to formalize the mathematical model of the helicopter, i.e. tangent bundle, Lie algebra and exponential map. Moreover, this chapter introduces a system of differential equations which will be used to describe the motion of the helicopter.
- *Chapter 3* introduces the structure of the helicopter, the reference systems and the forces used to write the mathematical model, e.g. the thrust of the rotors and the weight. In addition, in this chapter is performed the calculus to achieve the equations of motion starting from the Lagrangian function.
- *Chapter 4* presents the numerical approximation of the system of equations found in the chapter 3 using the *fEul* method. Then the fourth chapter introduces a tailored *fEul* method for  $SO(3)$ .
- *Chapter 5* introduces a helicopter type and shows all the values required to perform the simulation analysis. These values are presented in tables and figures and have been gathered from data-sheets.
- *Chapter 6* illustrates eight simulations and the linked resulting graphs. Each simulation is particularly focused on a input response, i.e. pitch response, roll response. The graphs contain all the information needed to know the response of the input given with respect to the simulation time.

---

# The

# Lagrange-d'Alembert-Pontryagin principle and the forced Euler-Poincaré equation

In this paper, we consider non-conservative non-linear dynamical systems whose state space  $\mathbb{G}$  possesses the mathematical structure of a *Lie group*.

## 2.1 Definition and properties

Let us recapitulate the following definitions and properties [13, 14] (see also [15, 16] for a non-strictly mathematical viewpoint):

**Matrix Lie group:** A smooth matrix manifold  $\mathbb{G}$  that is also an algebraic group is termed a matrix Lie group. A matrix group is a matrix-set endowed with an associative binary operation, termed *group multiplication* which, for any two elements  $g, h \in \mathbb{G}$ , is denoted by  $gh$  and endowed with the property of closure, an *identity element* with respect to the multiplication, denoted by  $e$ , such that  $eg = ge = g$  for any  $g \in \mathbb{G}$ , and an *inversion* operation, denoted by  $g^{-1}$ , with respect to multiplication, such that  $g^{-1}g = gg^{-1} = e$  for any  $g \in \mathbb{G}$ . A *left translation*  $L : \mathbb{G} \times \mathbb{G} \rightarrow \mathbb{G}$  is defined as  $L_g(h) := g^{-1}h$ . An instance of matrix Lie group is  $SO(3) := \{R \in \mathbb{R}^{3 \times 3} \mid R^\top R = RR^\top = I_3, \det(R) = +1\}$ , where the symbol  $^\top$  denotes matrix transposition and the quantity  $I_3$  represents a  $3 \times 3$  identity matrix.

**Tangent bundle and its metrization:** Given a point  $g \in \mathbb{G}$ , the tangent space to  $\mathbb{G}$  at  $g$  will be denoted as  $T_g\mathbb{G}$ . The tangent bundle associated with a manifold-group  $\mathbb{G}$  is denoted by  $T\mathbb{G}$  and plays the role of phase-space for a dynamical system whose state-space is  $\mathbb{G}$ . The inner product of two tangent vectors  $\xi, \eta \in T_g\mathbb{G}$  is denoted by  $\langle \xi, \eta \rangle_g$ . A smooth

function  $F : \mathbb{G} \rightarrow \mathbb{G}$  induces a linear map  $dF_g : T_g\mathbb{G} \rightarrow T_{F(g)}\mathbb{G}$  termed *pushforward map*. For a matrix Lie group, the pushforward map  $d(L_g)_h : T_h\mathbb{G} \rightarrow T_{g^{-1}h}\mathbb{G}$  associated to a left translation is  $d(L_g)_h(\eta) := g^{-1}\eta$ , with  $\eta \in T_h\mathbb{G}$ .

**Lie algebra:** The tangent space  $\mathfrak{g} := T_e\mathbb{G}$  to a Lie group at the identity is termed *Lie algebra*. The Lie algebra is endowed with *Lie brackets*, denoted as  $[\cdot, \cdot] : \mathfrak{g} \times \mathfrak{g} \rightarrow \mathfrak{g}$ , and an *adjoint endomorphism*  $\text{ad}_\xi \eta := [\xi, \eta]$ . The Lie algebra associated to the group  $\text{SO}(3)$  is  $\mathfrak{so}(3) := \{\xi \in \mathbb{R}^{3 \times 3} \mid \xi + \xi^\top = 0\}$ . On a matrix Lie algebra, the Lie brackets coincide with matrix commutator, namely  $[\xi, \eta] := \xi\eta - \eta\xi$ . The matrix commutator in  $\mathfrak{so}(3)$  is an anti-symmetric bilinear form, namely  $[\xi, \eta] + [\eta, \xi] = 0$ . A pushforward map  $d(L_g)_g : T_g\mathbb{G} \rightarrow \mathfrak{g}$  is denoted as  $dL_g$  for brevity. Given a smooth function  $\ell : \mathfrak{g} \rightarrow \mathbb{R}$ , for a matrix Lie group one may define the *fiber derivative* of  $\ell$ ,  $\frac{\partial \ell}{\partial \xi} \in \mathfrak{g}$ , at  $\xi \in \mathfrak{g}$  as the unique algebra element such that  $\left\langle \frac{\partial \ell}{\partial \xi}, \eta \right\rangle_e = \text{tr}((\mathbf{J}_\xi \ell)^\top \eta)$  for any  $\eta \in \mathfrak{g}$ , where  $\mathbf{J}_\xi \ell$  denotes the Jacobian \* matrix of the function  $\ell$  with respect to the matrix  $\xi$ .

**Exponential map:** Given a point  $g \in \mathbb{G}$  and a tangent vector  $v \in T_g\mathbb{G}$ , the *exponential* maps  $g$  to a point  $\exp_x(v)$ , namely it flows the point  $g$  along a geodesic line departing from  $g$  with initial direction  $v$ . On a matrix Lie group endowed with the Euclidean metric, it holds that  $\exp_g(v) = g\text{Exp}(g^{-1}v)$ , where  $\text{Exp}$  denotes a matrix exponential.

## 2.2 The Euler-Poincaré equations

The Lagrange-d'Alembert-Pontryagin (LDAP) principle is one of the fundamental concepts in mathematical physics to describe the time-evolution of the state of a physical system and to handle non-conservative external forces. The state-variables of the system are subjected to holonomic constraints, which are embodied in the structure of the state Lie group  $\mathbb{G}$ . These external forces often arise as control actions designed with the aim to driving the physical system into a predefined state [2]. Let  $\Lambda : T\mathbb{G} \rightarrow \mathbb{R}$  denote a Lagrangian function and  $F : T\mathbb{G} \rightarrow T\mathbb{G}$  a generalized force field<sup>†</sup>. The LDAP principle affirms that a dynamical system follows a trajectory  $g : [a, b] \rightarrow \mathbb{G}$  such that:

$$\delta \int_a^b \Lambda(g(t), \dot{g}(t)) dt + \int_a^b \langle F(g(t), \dot{g}(t)), \delta g(t) \rangle_{g(t)} dt = 0, \quad (2.1)$$

The left-most integral is called *action* and the symbol  $\delta$  denotes variation, namely the change of the action value from a trajectory  $g$  to a trajectory that is infinitely close to  $g$ , whose point-by-point change is denoted as  $\delta g$ . The variation *vanishes at endpoints* and is elsewhere *arbitrary*. In the above expression, an over-dot (as in  $\dot{g}$ ) denotes derivation with respect to the parameter  $t$ . The vanishing of the first term alone is called principle of stationary action. The right-most integral represents the total work done by the force field  $F$  due to the variation.

\*Notice that  $\mathbf{J}_\xi \ell$  is a formal Jacobian, namely a matrix of partial derivatives with respect of each entry of the matrix  $\xi$  without any regard of the internal summary of the matrix  $\xi$  itself.

<sup>†</sup>A generalized force field is generally taken as a smooth map from  $T\mathbb{G}$  to its dual  $T^*\mathbb{G}$  or, for left-invariant force fields, from an algebra  $\mathfrak{g}$  to its dual  $\mathfrak{g}^*$ . We adopt a non-standard definition because it eases the notation and is more easily translated into implementation.

A variational formulation is based on a continuous family of curves  $g : U \subset \mathbb{R}^2 \rightarrow \mathbb{G}$ , where each element is denoted as  $g(t, \varepsilon)$ . The index  $\varepsilon$  selects a curve in the family, and the index  $t$  individuates a point over this curve. All the curves in the family depart from the same initial point and arrive at the same endpoint, namely,  $g(a, \varepsilon)$  and  $g(b, \varepsilon)$  are constant with respect to  $\varepsilon$ . The variations in (2.1) are defined as

$$\delta \int_a^b \Lambda(g, \dot{g}) dt := \int_a^b \frac{\partial}{\partial \varepsilon} \Lambda(g(t, \varepsilon), \dot{g}(t, \varepsilon)) dt \Big|_{\varepsilon=0}, \quad \delta g(t) := \frac{\partial g(t, \varepsilon)}{\partial \varepsilon} \Big|_{\varepsilon=0}. \quad (2.2)$$

The following result, enunciated directly for matrix Lie groups, is of prime importance, as it relates a variation of velocity to velocity of variation. *Lemma1:* [[17]] Given a smooth function  $g : U \subset \mathbb{R}^2 \rightarrow \mathbb{G}$  on a matrix Lie group, define:

$$\xi(t, \varepsilon) := g^{-1}(t, \varepsilon) \frac{\partial g(t, \varepsilon)}{\partial t}, \quad \eta(t, \varepsilon) := g^{-1}(t, \varepsilon) \frac{\partial g(t, \varepsilon)}{\partial \varepsilon}. \quad (2.3)$$

A variation of a trajectory induces a variation of its velocity field given by

$$\frac{\partial \xi}{\partial \varepsilon} = \dot{\eta} + \text{ad}_\xi \eta. \quad (2.4)$$

Assuming that the Lagrangian as well as the generalized force field  $F$  are left invariant, we may write  $\Lambda(g, \dot{g}) = \ell(g^{-1}\dot{g})$  and  $g^{-1}F(g, \dot{g}) = f(g^{-1}\dot{g})$ , where  $\ell : \mathfrak{g} \rightarrow \mathbb{R}$  and  $f : \mathfrak{g} \rightarrow \mathfrak{g}$  denote a *reduced Lagrangian* and a *reduced force field*, respectively. In addition, if the inner product is left-invariant, it holds that

$$\langle F(g, \dot{g}), \delta g \rangle_g = \langle f(g^{-1}\dot{g}), g^{-1}\delta g \rangle_e. \quad (2.5)$$

Therefore, the LDPA principle (2.1) reduces to

$$\delta \int_a^b \ell(g^{-1}\dot{g}) dt + \int_a^b \langle f(g^{-1}\dot{g}), g^{-1}\delta g \rangle_e dt = 0, \quad (2.6)$$

where it is legitimate to replace  $g^{-1}\dot{g}$  with  $\xi$  and  $g^{-1}\delta g$  with  $\eta$  and then set  $\varepsilon$  to 0.

By means of the Lemma 2.2, the variational formulation of the reduced LDPA principle may be converted into a differential-equations form. [[17]] Let  $\xi := g^{-1}\dot{g}$  and  $\eta := g^{-1}\delta g$ . The solution of the integral Lagrange-d'Alembert equation (2.6) under perturbations of the form  $\frac{\partial \xi}{\partial \varepsilon} = \dot{\eta} + \text{ad}_\xi \eta$ , which vanishes at endpoints, satisfies the Euler-Poincaré equation

$$\frac{d}{dt} \frac{\partial \ell}{\partial \xi} = \text{ad}_\xi^* \left( \frac{\partial \ell}{\partial \xi} \right) + f, \quad (2.7)$$

where  $\text{ad}^*$  denotes the adjoint of the operator  $\text{ad}$  with respect to the inner product of  $\mathfrak{g}$ <sup>‡</sup>.

The complete system of differential equations then read

$$\begin{cases} \dot{g} &= g\xi, \\ \frac{d}{dt} \frac{\partial \ell}{\partial \xi} &= \text{ad}_\xi^* \left( \frac{\partial \ell}{\partial \xi} \right) + f. \end{cases} \quad (2.8)$$

---

<sup>‡</sup>The adjoint  $\omega^*$  of an operator  $\omega : \mathfrak{g} \rightarrow \mathfrak{g}$  with respect to an inner product  $\langle \cdot, \cdot \rangle$  satisfies by  $\langle \omega(\xi), \eta \rangle = \langle \xi, \omega^*(\eta) \rangle$ .

The above equations will be used to describe the rotational component of motion of a flying object like a helicopter or a drone. The forcing term takes into account several *external* driving phenomena, such as

**Energy dissipation:** Energy dissipation is due, e.g., to friction with air particles. For instance, a linear dissipation term represents aerodynamic drag.

**Control actions:** Other than dissipation (which is often neglected in simplistic models), the forcing term depends on the problem under investigation. It might serve to incorporate into the equations control terms aimed, for instance, at stabilizing the motion or to drive a dynamical system [18].

## 2.3 Exemplary case: Euclidean space

In order to clarify the physical meaning of the Euler-Poincaré equations, let us recall the classical version of these equations for the space  $\mathbb{R}^n$ , which is also instrumental in describing the translational component of motion of a flying device. The principle (2.1) on  $\mathbb{R}^n$ , endowed with the Euclidean inner product, reads:

$$\delta \int_a^b \Lambda(p(t), \dot{p}(t)) dt + \int_a^b f(p(t), \dot{p}(t))^\top \delta p(t) dt = 0, \quad (2.9)$$

where  $\Lambda : \mathbb{R}^n \times \mathbb{R}^n \rightarrow \mathbb{R}$  denotes a Lagrangian function,  $p = p(t)$  a trajectory on  $\mathbb{R}^n$  and  $f : \mathbb{R}^n \times \mathbb{R}^n \rightarrow \mathbb{R}^n$  a non-conservative force field. Upon computing the variation, we get

$$\int_a^b \left( \left( \frac{\partial \Lambda}{\partial p} \right)^\top \delta p + \left( \frac{\partial \Lambda}{\partial \dot{p}} \right)^\top \delta \dot{p} + f^\top \delta p \right) dt = 0. \quad (2.10)$$

Integrating by parts the second term and recalling that the variations vanish at the end-points, we get

$$\int_a^b \left( \frac{\partial \Lambda}{\partial p} - \frac{d}{dt} \frac{\partial \Lambda}{\partial \dot{p}} + f \right)^\top \delta p dt = 0. \quad (2.11)$$

Since the variation  $\delta p$  is arbitrary, the dynamics of the variable  $p$  is governed by the equation

$$\frac{d}{dt} \frac{\partial \Lambda}{\partial \dot{p}} = \frac{\partial \Lambda}{\partial p} + f. \quad (2.12)$$

## Mathematical model of a helicopter

This section introduces a helicopter model based on the Lie group  $\mathbb{G} := \text{SO}(3)$  of 3-dimensional rotations  $R$ .

Since, in the state space  $\mathbb{G} := \text{SO}(3)$ , it holds that  $(dL_R)^{-1}(\xi) = R\xi$  and  $\text{ad}_\xi^* \eta = -\text{ad}_\xi \eta$  [17], the Euler-Poincaré equations read

$$\begin{cases} \dot{R} = R\xi, \\ \frac{d}{dt} \frac{\partial \ell}{\partial \xi} = -\text{ad}_\xi \left( \frac{\partial \ell}{\partial \xi} \right) + \tau, \end{cases} \quad (3.1)$$

where  $\tau$  denotes the resultant of all external *mechanical torques*. In this context, the state variable  $R \in \text{SO}(3)$  denotes the *attitude* of a rigid body (i.e., its orientation with respect to a earth-fixed reference frame) and the state-variable  $\xi \in \mathfrak{so}(3)$  denotes its *instantaneous angular velocity*. Moreover, the quantity  $\mu := \frac{\partial \ell}{\partial \xi}$  represents an angular momentum and the second Euler-Poincaré equation reads  $\dot{\mu} = [\mu, \xi] + \tau$ , which is a generalization of the well-known angular momentum theorem, where the term  $[\mu, \xi]$  represents the inertial torque due to the internal mass unbalance of a body.

It is convenient to define the operator  $[\cdot] : \mathbb{R}^3 \rightarrow \mathfrak{g}$  as:

$$x := \begin{bmatrix} x_1 \\ x_2 \\ x_3 \end{bmatrix} \mapsto [x] := \begin{bmatrix} 0 & -x_3 & x_2 \\ x_3 & 0 & -x_1 \\ -x_2 & x_1 & 0 \end{bmatrix}. \quad (3.2)$$

Since any skew-symmetric matrix in  $\mathfrak{so}(3)$  may be written as in (3.2), it is convenient to define a basis of  $\mathfrak{so}(3) = \text{span}(\xi_x, \xi_y, \xi_z)$  as follows:

$$\xi_x := \begin{bmatrix} 0 & 0 & 0 \\ 0 & 0 & -1 \\ 0 & 1 & 0 \end{bmatrix}, \quad \xi_y := \begin{bmatrix} 0 & 0 & 1 \\ 0 & 0 & 0 \\ -1 & 0 & 0 \end{bmatrix}, \quad \xi_z := \begin{bmatrix} 0 & -1 & 0 \\ 1 & 0 & 0 \\ 0 & 0 & 0 \end{bmatrix}. \quad (3.3)$$

In order to shorten some relations, it is also convenient to introduce the *matrix anti-commutator*  $\{A, B\} := AB + BA$ . Moreover, some relations take advantage of the skew-



symmetric projection  $\{\{\cdot\}\} : \mathbb{R}^{3 \times 3} \rightarrow \mathfrak{so}(3)$ , defined as  $\{\{A\}\} := \frac{1}{2}(A - A^\top)$ . It also pays to define the ‘diag’ operator as  $\text{diag}(a, b, c) := \begin{bmatrix} a & 0 & 0 \\ 0 & b & 0 \\ 0 & 0 & c \end{bmatrix}$ .

In the present setting, we equip the algebra  $\mathfrak{so}(3)$  with the canonical metric  $\langle \xi, \eta \rangle_e := \text{tr}(\xi^\top \eta)$ . With this choice, the fiber derivative of a scalar function  $\ell : \mathfrak{so}(3) \rightarrow \mathbb{R}$  takes a special form. [[19]] The fiber derivative of a scalar function  $\ell : \mathfrak{so}(3) \rightarrow \mathbb{R}$  takes the form

$$\frac{\partial \ell}{\partial \xi} = \frac{1}{2}(\mathbf{J}_\xi \ell - \mathbf{J}_\xi^\top \ell) \in \mathfrak{so}(3). \quad (3.4)$$

It is immediate to verify that the fiber derivative corresponds to the orthogonal projection of the Jacobian into the algebra  $\mathfrak{g}$ , namely  $\frac{\partial \ell}{\partial \xi} = \{\{\mathbf{J}_\xi \ell\}\}$ . Moreover, it is convenient to recall a property of the matrix ‘trace’ operator, namely the cyclic permutation property  $\text{tr}(ABC) = \text{tr}(BCA) = \text{tr}(CAB)$  for any square matrices  $A, B, C$ .

Modeling a complex object to get the differential equations that describe its rotational and translational dynamics consists essentially in

- defining a Lagrangian function  $\ell$  on the basis of the kinetic and potential energy of its components, which accounts for the geometrical and mechanical features of each component;
- computing the total mechanical torque  $\tau$  exerted by the moving parts on the body of the complex object.

These descriptors, for a helicopter, will be evaluated in the next sections.

### 3.1 Model of a helicopter with a single principal rotor and a tail rotor

In order to formalize the behaviour of a helicopter into a mathematical model, let us assume the existence of an inertial (earth) reference frame  $\mathcal{F}_E$ . Also, it is necessary to establish a body-fixed reference frame  $\mathcal{F}_B$ , as shown in Figure 3.1: the origin of the reference frame  $\mathcal{F}_B$  is located at the centre of gravity of the helicopter and the three axes coincide with its principal inertia axes. The thrust  $\varphi_m$  exerted by the principal rotor appears at the tip of the helicopter’s body, which is located along the  $z$ -axis at a distance  $D_m$  from the centre of gravity, whereas the thrust  $\varphi_t$  exerted by the tail rotor appears at the tail of the helicopter’s body, which is located along the  $-x$  axis at a distance  $D_t$  from the centre of gravity.

The term  $\frac{1}{2}u_m$  represents the intensity of the thrust exerted by the main rotor,  $\frac{1}{2}u_t$  is the one exerted by the tail rotor, both are expressed in Newtons (N). Considering the total thrust  $\varphi := \varphi_t + \varphi_m$  as a vector, a *collective control* management of the main rotor results in a change of the thrust’s intensity exerted, therefore a change in  $u_m$ , whereas a *cyclic*

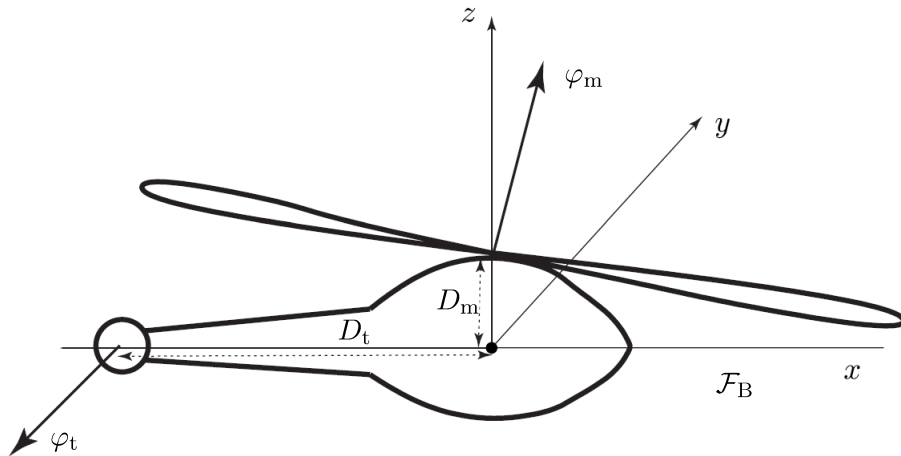


Figure 3.1: Schematic of a helicopter with a principal rotor and a tail rotor (adapted from [2]). (The principal rotor to centre of mass distance  $D_m$  and the tail rotor to centre of mass distance  $D_t$  are expressed in meters (m)).

*control* management changes the direction of the lift exerted, therefore the pitch angle  $\alpha_p$  (in radians (rad)) and the sideways roll angle  $\alpha_r$  (in radians).

The expressions of the thrusts (from [2]) and of their moment arms in the helicopter's body-fixed frame  $\mathcal{F}_B$  are given by

$$\varphi_m := \frac{1}{2}u_m \begin{bmatrix} \sin \alpha_p \cos \alpha_r \\ -\sin \alpha_r \\ \cos \alpha_p \cos \alpha_r \end{bmatrix}, \quad b_m := \begin{bmatrix} 0 \\ 0 \\ D_m \end{bmatrix}, \quad (3.5)$$

$$\varphi_t := \frac{1}{2}u_t \begin{bmatrix} 0 \\ -1 \\ 0 \end{bmatrix}, \quad b_t := \begin{bmatrix} -D_t \\ 0 \\ 0 \end{bmatrix}. \quad (3.6)$$

Where, the vector  $\frac{2\varphi_m}{u_m}$  denotes the unit normal to the *rotor disk* [10].

Concerning the thrust generated by the principal rotor, we may notice what follows:

- whenever  $\alpha_r = \alpha_p = 0$ , the thrust takes the expression  $\frac{1}{2}u_m \begin{bmatrix} 0 \\ 0 \\ 1 \end{bmatrix}$ , namely, only the  $z$ -component is non-null and the thrust is vertical, which may cause pure vertical translation;
- whenever  $\alpha_p = 0$  and  $\alpha_r \neq 0$ , the thrust takes the expression  $\frac{1}{2}u_m \begin{bmatrix} 0 \\ -\sin \alpha_r \\ \cos \alpha_r \end{bmatrix}$ , namely, the  $x$ -component is null and the thrust belongs to the  $y-z$  plane, as shown in Figure 3.2, hence it may only produce a rotation along the  $x$ -axis, which corresponds to pure rolling; *Remark:* Using the right-hand law a counter clock wise turning is consider positive

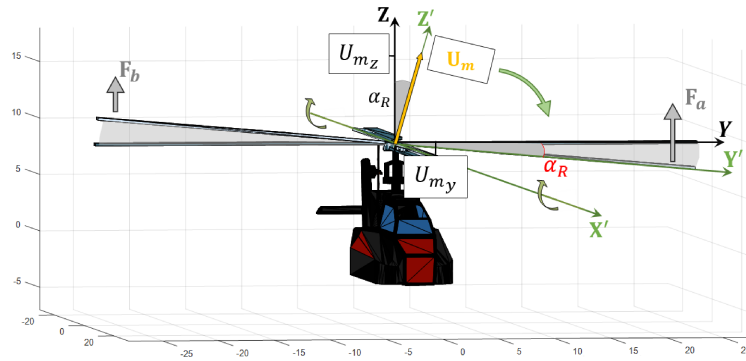


Figure 3.2: Variation of the angle of attack along  $x$  axis.

- whenever  $\alpha_r = 0$  and  $\alpha_p \neq 0$ , the thrust takes the expression  $\frac{1}{2}u_m \begin{bmatrix} \sin \alpha_p \\ 0 \\ \cos \alpha_p \end{bmatrix}$ , namely, the  $y$ -component is null and the thrust belongs to the  $x-z$  plane, as shown in Figure 3.3, hence it may only produce a rotation along the  $y$ -axis, which corresponds to pure pitching.

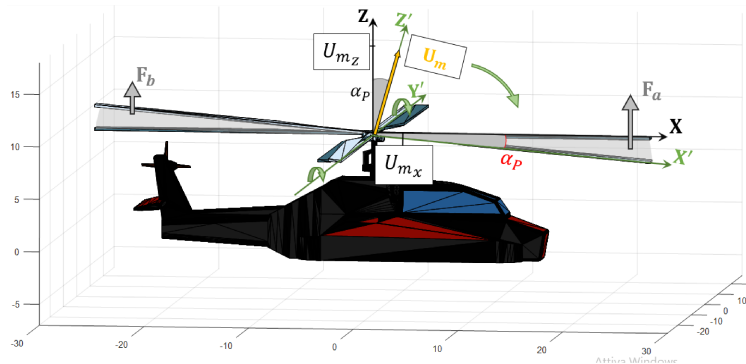


Figure 3.3: Variation of the angle of attack along the  $y$ -axis.

- whenever the thrust belongs, if the outcome is not a pure rolling or pure pitching, then the non-vertical projection of  $u_m$  belongs to  $x-y$  plane and therefore is a combination of  $\cos(\alpha_p) \cos(\alpha_r)$ . As a consequence,  $\varphi_m$  takes the standard form in the equation (3.5).

Notice that the inclination of the blades influences the thrust and the torque acting on the fuselage, but does not influence directly the roll and the pitch attitude of the helicopter.

Also, notice that the thrust  $\frac{1}{2}u_m$  does not distribute equally across the three directions of the space and, in particular, that a change in the angles of attack of the blades weakens the vertical component of the thrust: when a helicopter tilts, it tends to fall, unless the thrust is compensated by the pilot. It is also worth noticing that the total thrust  $\varphi$  acting on the fuselage has a  $y$  component that depends on the tail rotor thrust. This component

causes the translation of the helicopter in the direction of  $\varphi_t$ : this is called drift effect (or translation tendency).

The mechanical torque exerted by the two rotors on the helicopter's fuselage, expressed in N·m is termed active torque and is given by

$$\begin{aligned}\tau_{\mathcal{A}} &:= \frac{1}{2} (\varphi_m b_m^\top - b_m \varphi_m^\top + \varphi_t b_t^\top - b_t \varphi_t^\top) \\ &= \frac{1}{2} \begin{bmatrix} 0 & -D_t u_t & D_m u_m \sin \alpha_p \cos \alpha_r \\ D_t u_t & 0 & -D_m u_m \sin \alpha_r \\ -D_m u_m \sin \alpha_p \cos \alpha_r & D_m u_m \sin \alpha_r & 0 \end{bmatrix}. \quad (3.7)\end{aligned}$$

The mechanical torque due to the drag of the principal rotor, namely the resultant of the torque that tends to make the helicopter spin as a counter-reaction to the spinning of the rotor, expressed in N·m, may be quantify by

$$\tau_{\mathcal{D}} := -\frac{1}{2} \gamma u_m \xi_z, \quad (3.8)$$

where  $\gamma > 0$  is termed *air drag* coefficient (whose measurement unit is meters) and represents the efficacy with which the air surrounding the helicopter pushes the rotor as a reaction of its spinning.

According to the canonical basis (3.3), the total mechanical torque  $\tau := \tau_{\mathcal{A}} + \tau_{\mathcal{D}}$  may be decomposed as  $\tau = \tau_x \xi_x + \tau_y \xi_y + \tau_z \xi_z$ , with

$$\begin{cases} \tau_x = \frac{1}{2} D_m u_m \sin \alpha_r, \\ \tau_y = \frac{1}{2} D_m u_m \sin \alpha_p \cos \alpha_r, \\ \tau_z = \frac{1}{2} D_t u_t - \frac{1}{2} \gamma u_m. \end{cases} \quad (3.9)$$

The component  $\tau_x$  is responsible for the rolling of the helicopter (plane  $y - z$ ), the component  $\tau_y$  is responsible for the pitching of the helicopter (plane  $x - z$ ). The component  $\tau_z$  is responsible for the control of the yawing of the helicopter (plane  $x - y$ ): to prevent the spinning of the aircraft, it is necessary to control the thrust  $u_t$  of the tail rotor in such a way that  $D_t u_t - \gamma u_m \approx 0$ . During hovering, the vertical component of the total thrust needs to balance the weight force of the helicopter.

According to the specialized literature (see, e.g., [20]), the maximum value of the thrust  $u$  of a rotor (in Newtons) may be computed by the expression

$$u := \frac{1}{2} C_u \rho A (l_{\mathcal{R}} \Omega_m)^2, \quad (3.10)$$

where  $C_u$  is a (dimensionless) thrust coefficient that represents the efficiency of the rotor,  $\rho$  represents the density of the air at a given temperature and altitude in  $\text{kg}\cdot\text{m}^{-3}$ ,  $A$  denotes the area of the rotor disk, in  $\text{m}^2$ , which contributes to generating the thrust,  $l_{\mathcal{R}}$  represents the radius of the rotor disk (namely, the length of a blade) in meters and  $\Omega_m$  denotes the angular velocity of the rotor in  $\text{rad}\cdot\text{s}^{-1}$ . In fact, the product  $l_{\mathcal{R}} \Omega_m$  denotes the tip velocity of a blade. The thrust may be expressed as  $u = \beta_u \Omega_m^2$ , with  $\beta_u := \frac{\pi}{2} C_u \rho l_{\mathcal{R}}^4$ .

Besides, the mechanical power (in Watts) that the engine transfers to the rotor is given by

$$w := \frac{1}{2} C_w \rho A (l_{\mathcal{R}} \Omega_m)^2 \Omega_m, \quad (3.11)$$

where  $C_w$  denotes a (dimensionless) power coefficient. The power may be expressed as a cubic function of the rotor speed, namely  $w = \beta_w \Omega_m^3$ .

The main rotor disk area  $A$  changes its value thanks to *collective control* and consequently to  $\alpha_c$ . In fact,  $A$ 's value is related to the portion of each blade that pushes the helicopter, for instance, upward. In order to describe correctly the area of the disk that contributes to generating thrust, it is assumed  $A = \pi l_R^2 \sin \alpha_c$ . Therefore, if the blades are considered with no thickness, no built-in twists and perfectly horizontal, namely in the earth inertial reference's  $x - y$  plane, then when  $\alpha_c = 0$  the helicopter has no thrust. Instead, when all blades have an angle  $\alpha_c > 0$  the thrust is no longer null and the turning of the blades produces a vertical thrust that tends to counteract the helicopter's weight force. The equation (3.10) becomes:

$$u := \frac{1}{2} C_u \rho \pi l_R^4 \Omega_m^2 \sin \alpha_c, \quad (3.12)$$

with  $\alpha_c \in [\alpha_{c,\min}, \alpha_{c,\max}]$ . The minimum and the maximum value of the thrust depend on the range of the angle of attack (Aof) of the principal rotors blades, whereas the range of Aof is related to the shape and the built-in twist of the blades, besides the swash-plate rods mobility. The power coefficient  $C_w$  is related to the thrust coefficient  $C_u$  by the relationship

$$C_w = \frac{C_u^{3/2}}{\sqrt{2}}. \quad (3.13)$$

The mechanical power  $w$  absorbed by the helicopter's engine at the reference speed of 100% is usually provided by data-sheets. Considering  $w$  as known it is possible to calculate the power and the thrust coefficients, that otherwise would have to be measured through experiments on the real engine. The value of the first coefficient, following the equation (3.11), is

$$C_w = \frac{2w}{\rho A (l_R \Omega_m)^2 \Omega_m} \quad (3.14)$$

Consequently it is possible to find the value of  $C_u$  using the equation (3.13). Taking into account the possible redundancy of indexes, the expression (3.12) is written explicitly for the main rotor fixing  $u = u_m$ , while a similar expression may describe the thrust exerted by the tail rotor. Thus, the equation below based on tail rotor characteristics:

$$u_t := \frac{1}{2} C_u^T \rho \pi l_T^4 \Omega_t^2 \sin \alpha_c^T, \quad (3.15)$$

Where  $C_u^T$  is the thrust coefficient of the tail rotor and  $l_T$  is the radius of the tail rotor's blade.

The drag coefficient is generally unknown, but it is possible to estimate its value by assuming (1) the helicopter hovering, and (2) that the mechanical torque of the tail rotor balances the undesired drag torque which would tend to make the helicopter yawing. Indeed, in hovering condition, with the tail rotor's blades collective angle at a value half of its interval range  $\alpha_{c,\text{mid}}^T := \frac{\alpha_{c,\min}^T + \alpha_{c,\max}^T}{2}$  (see Table 5.1) and at 100% of the tail rotor speed, the helicopter should have no yawing. The drag coefficient could be found by the condition  $e_z^T \tau = 0$  as

$$\gamma = D_t \frac{C_u l_R^4 \Omega_m^2 \sin \alpha_c}{C_u^T l_T^4 \Omega_t^2 \sin \alpha_{c,\text{mid}}^T}. \quad (3.16)$$

Where  $e_z := [0 \ 0 \ 1]^T$ .

## 3.2 Lagrangian function associated to the helicopter model

To complete the motion dynamics, it is necessary to write explicitly the Lagrangian function of the helicopter, which coincides with its kinetic energy minus its potential energy, both expressed in the inertial reference frame  $\mathcal{F}_E$ .

**Kinetic energy of the fuselage:** The position of the centre of gravity of the helicopter in the inertial reference frame  $\mathcal{F}_E$  at time  $t$  is denoted as  $p(t)$ . The position of each infinitesimal volume of the body in the body-fixed frame  $\mathcal{F}_B$  is denoted by  $s$ . Since the helicopter's fuselage is rigid, the position of each volume element, at time  $t$ , is  $p(t) + R(t)s$ , where  $R(t) \in \text{SO}(3)$  denotes a rotation matrix that takes the body-fixed frame  $\mathcal{F}_B$  to coincide with  $\mathcal{F}_E$ . The kinetic energy of the helicopter's body  $\mathcal{B}$  with respect to the inertial reference frame  $\mathcal{F}_E$  may be written as

$$\ell_{\mathcal{B}} := \frac{1}{2} \int_{\mathcal{B}} \left\| \frac{d(p + Rs)}{dt} \right\|^2 dm = \frac{1}{2} \int_{\mathcal{B}} \|\dot{p} + \dot{R}s\|^2 dm, \quad (3.17)$$

where  $dm$  denotes the mass content of the infinitesimal volume. Recalling that  $\dot{R} = R\xi$ , with  $\xi \in \mathfrak{so}(3)$ , we get:

$$\begin{aligned} \ell_{\mathcal{B}} &= \frac{1}{2} \int_{\mathcal{B}} \text{tr}((\dot{p} + \dot{R}s)(\dot{p} + \dot{R}s)^\top) dm = \frac{1}{2} \int_{\mathcal{B}} \text{tr}(\dot{p}\dot{p}^\top + R\xi s s^\top \xi^\top R^\top + 2\dot{p}s^\top \dot{R}) dm \\ &= \frac{1}{2} M_{\mathcal{B}} \|\dot{p}\|^2 + \frac{1}{2} \text{tr}(R\xi \hat{J}_{\mathcal{B}} \xi^\top R^\top) + M_{\mathcal{B}} \text{tr}(\dot{p} c_{\mathcal{B}}^\top \dot{R}), \end{aligned} \quad (3.18)$$

where  $\text{tr}(\cdot)$  denotes matrix trace, the cancellation is due to the cyclic permutation property of the trace operator and to the defining property of rotations ( $R^\top R = I_3$ ). The constant quantities that appear in the expression (3.18) are defined as follows

$$M_{\mathcal{B}} := \int_{\mathcal{B}} dm > 0, \quad c_{\mathcal{B}} := \frac{1}{M_{\mathcal{B}}} \int_{\mathcal{B}} s dm \in \mathbb{R}^3, \quad \hat{J}_{\mathcal{B}} := \int_{\mathcal{B}} s s^\top dm \in \mathbb{R}^{3 \times 3}. \quad (3.19)$$

The quantity  $M_{\mathcal{B}}$  denotes the total mass of the helicopter's fuselage. The matrix  $\hat{J}_{\mathcal{B}}$  denotes a *non-standard inertia tensor* [21]. The *standard inertia tensor* of the helicopter's body is defined as

$$J_{\mathcal{B}} := \int_{\mathcal{B}} \llbracket s \rrbracket \llbracket s \rrbracket^\top dm. \quad (3.20)$$

These inertia tensors are related by the following result: *Lemma2:* [[21]] The non-standard moment of inertia  $\hat{J}$  of a body is related to its standard moment of inertia  $J$  by the relationship  $\hat{J} = \frac{1}{2} \text{tr}(J) I_3 - J$ .

Assuming that the shape of the fuselage may be assimilated to an ellipsoid, its standard inertial tensor takes the form:

$$J_{\mathcal{B}} = \begin{bmatrix} \frac{M_{\mathcal{B}}(b^2+c^2)}{5} & 0 & 0 \\ 0 & \frac{M_{\mathcal{B}}(a^2+c^2)}{5} & 0 \\ 0 & 0 & \frac{M_{\mathcal{B}}(a^2+b^2)}{5} \end{bmatrix}, \quad (3.21)$$

where  $a, b, c$  denote the semi-axes lengths ( $a$  refers to the  $x$ -axis,  $b$  refers to the  $y$ -axis and  $c$  refers to the  $z$ -axis). The non-standard inertial tensor of the fuselage reads

$$\hat{J}_{\mathcal{B}} = \begin{bmatrix} \frac{M_{\mathcal{B}} a^2}{5} & 0 & 0 \\ 0 & \frac{M_{\mathcal{B}} b^2}{5} & 0 \\ 0 & 0 & \frac{M_{\mathcal{B}} c^2}{5} \end{bmatrix}. \quad (3.22)$$

Since the origin of the reference frame  $\mathcal{F}_{\mathcal{B}}$  coincides with the centre of gravity of the aircraft, not of the fuselage alone, in general it holds that the centre of mass of the fuselage  $c_{\mathcal{B}} \neq 0$ , therefore

$$\ell_{\mathcal{B}} = \frac{1}{2} M_{\mathcal{B}} \|\dot{p}\|^2 + \frac{1}{2} \text{tr}(\xi \hat{J}_{\mathcal{B}} \xi^{\top}) + M_{\mathcal{B}} \text{tr}(\dot{p} c_{\mathcal{B}}^{\top} \xi^{\top} R^{\top}). \quad (3.23)$$

**Kinetic energy of the principal rotor:** The position of the centre of gravity of the principal rotor with respect to the reference frame  $\mathcal{F}_{\mathcal{B}}$  is individuated by the vector  $b_m$  defined in (3.5). A reference frame  $\mathcal{F}_{\mathcal{R}}$  whose  $z$ -axis coincides with the  $z$ -axis of the reference frame  $\mathcal{F}_{\mathcal{B}}$  is associated to the rotor. Hence the position of each volume element in the principal rotor  $\mathcal{R}$  at time  $t$  in the inertial reference frame  $\mathcal{F}_{\mathcal{E}}$  is  $p(t) + R(t)(b_m + R_m(t)s)$ , where  $R_m \in \text{SO}(3)$  denotes the instantaneous orientation matrix of the principal rotor (rotation that aligns the rotor-fixed reference frame  $\mathcal{F}_{\mathcal{R}}$  to the body-fixed reference frame  $\mathcal{F}_{\mathcal{B}}$ ) and  $s$  denotes the position of a point of the rotor in a rotor-fixed reference frame. The matrix  $R_m$  represents a rotation about the  $z$ -axis of the reference frame  $\mathcal{F}_{\mathcal{R}}$ , hence it

takes the form  $\begin{bmatrix} \cos \theta_m & -\sin \theta_m & 0 \\ \sin \theta_m & \cos \theta_m & 0 \\ 0 & 0 & 1 \end{bmatrix}$ , therefore  $\dot{R}_m = \xi_m R_m$ , where  $\xi_m = \Omega_m \xi_z$  and  $\theta_m$  indicates the rotation angle of the main rotor.

The time-derivative of the position of each volume element is

$$\frac{d}{dt} [p + R(b_m + R_m s)] = \dot{p} + \dot{R}(b_m + R_m s) + R \dot{R}_m s = \dot{p} + R \xi b_m + R(\xi + \xi_m) R_m s. \quad (3.24)$$

The angular velocity matrix  $\xi_m \in \mathfrak{so}(3)$  of the principal rotor is controlled by the pilot and is hence a known quantity (although, as already underlined, most helicopters are designed to a fixed rotor speed). The kinetic energy per mass element  $dm$  of the principal rotor  $\mathcal{R}$  may be written as

$$\begin{aligned} & \frac{1}{2} \text{tr}([\dot{p} + \dot{R}b_m + R(\xi + \xi_m)R_m s][\dot{p} + \dot{R}b_m + R(\xi + \xi_m)R_m s]^{\top}) = \\ & \frac{1}{2} \|\dot{p}\|^2 + \frac{1}{2} \text{tr}(\mathcal{R} \xi b_m b_m^{\top} \xi^{\top} \mathcal{R}^{\top}) + \frac{1}{2} \text{tr}(\mathcal{R}(\xi + \xi_m)R_m s s^{\top} R_m^{\top}(\xi + \xi_m)^{\top} \mathcal{R}^{\top}) + \\ & \text{tr}(\dot{p} b_m^{\top} \xi^{\top} R^{\top}) + \text{tr}(\dot{p} s^{\top} R_m^{\top}(\xi + \xi_m)R^{\top}) + \text{tr}(\mathcal{R} \xi b_m s^{\top} R_m^{\top}(\xi + \xi_m)^{\top} \mathcal{R}^{\top}). \end{aligned} \quad (3.25)$$

The kinetic energy of the principal rotor  $\mathcal{R}$  in the earth frame  $\mathcal{F}_{\mathcal{E}}$  may thus be written as

$$\begin{aligned} \ell_{\mathcal{R}} = & \frac{1}{2} M_{\mathcal{R}} \|\dot{p}\|^2 + \frac{1}{2} M_{\mathcal{R}} \text{tr}(\xi b_m b_m^{\top} \xi^{\top}) + \frac{1}{2} \text{tr}((\xi + \xi_m) R_m \hat{J}_{\mathcal{R}} R_m^{\top} (\xi + \xi_m)^{\top}) + \\ & M_{\mathcal{R}} \text{tr}(\dot{p} b_m^{\top} \xi^{\top} R^{\top}) + M_{\mathcal{R}} \text{tr}(\dot{p} c_{\mathcal{R}}^{\top} R_m^{\top} (\xi + \xi_m) R^{\top}) + M_{\mathcal{R}} \text{tr}(\xi b_m c_{\mathcal{R}}^{\top} R_m^{\top} (\xi + \xi_m)^{\top}) \end{aligned} \quad (3.26)$$

where

$$M_{\mathcal{R}} := \int_{\mathcal{R}} dm > 0, \quad \hat{J}_{\mathcal{R}} := \int_{\mathcal{R}} s s^{\top} dm \in \mathbb{R}^{3 \times 3} \quad \text{and} \quad c_{\mathcal{R}} := \frac{1}{M_{\mathcal{R}}} \int_{\mathcal{R}} s dm \in \mathbb{R}^3. \quad (3.27)$$

In order to simplify the expression (3.26), we may assume that the principal rotor is perfectly symmetric about its centre of mass, which implies that  $c_{\mathcal{R}} = 0$ . Moreover, we may assume that the principal rotor may be schematized as two rods of mass  $\frac{1}{2}M_{\mathcal{R}}$  each and length  $2l_{\mathcal{R}}$ , one along the  $x$  axis and one along the  $y$ -axis, spinning around the  $z$ -axis, therefore:

$$J_{\mathcal{R}} = \begin{bmatrix} j_{\mathcal{R}} & 0 & 0 \\ 0 & j_{\mathcal{R}} & 0 \\ 0 & 0 & 2j_{\mathcal{R}} \end{bmatrix} \quad \text{that is } \hat{J}_{\mathcal{R}} = j_{\mathcal{R}} \text{diag}(1, 1, 0), \quad (3.28)$$

by Lemma 3.2, with  $j_{\mathcal{R}} := \frac{1}{12} \frac{M_{\mathcal{R}}}{2} (2l_{\mathcal{R}})^2 = \frac{1}{6} M_{\mathcal{R}} l_{\mathcal{R}}^2$ . A consequence is that the expression  $R_m \hat{J}_{\mathcal{R}} R_m^{\top}$  simplifies to  $\hat{J}_{\mathcal{R}}$ . Therefore, the kinetic energy of the principal rotor is given by

$$\ell_{\mathcal{R}} = \frac{1}{2} M_{\mathcal{R}} \|\dot{p}\|^2 + \frac{1}{2} M_{\mathcal{R}} \text{tr}(\xi b_m b_m^{\top} \xi^{\top}) + \frac{1}{2} \text{tr}((\xi + \xi_m) \hat{J}_{\mathcal{R}} (\xi + \xi_m)^{\top}) + M_{\mathcal{R}} \text{tr}(\dot{p} b_m^{\top} \xi^{\top} (\mathbf{R} \bar{\mathbf{2}} \mathbf{9}))$$

Rearranging these terms shows that the kinetic energy of the principal rotor may be written equivalently as the quadratic form

$$\ell_{\mathcal{R}} = \frac{1}{2} M_{\mathcal{R}} \|\dot{p} + R \xi b_m\|^2 + \frac{1}{2} \text{tr}((\xi + \xi_m) \hat{J}_{\mathcal{R}} (\xi + \xi_m)^{\top}), \quad (3.30)$$

where the first term represents the translational kinetic energy of the centre of mass of the principal rotor in the reference system  $\mathcal{F}_{\mathbb{E}}$ , whereas the second term represents the rotational kinetic energy of the principal rotor in the reference system  $\mathcal{F}_{\mathbb{E}}$ .

**Kinetic energy of the tail rotor:** The position of the tail rotor with respect to the reference frame  $\mathcal{F}_{\mathbb{B}}$  is individuated by the vector  $b_t$  defined in (3.6), hence the position of each point in the tail rotor  $\mathcal{T}$  at time  $t$  is  $p(t) + R(t)(b_t + R_t(t)s)$ , where  $R_t \in \text{SO}(3)$  denotes the instantaneous orientation matrix of the rotor with respect to a body-fixed reference frame  $\mathcal{F}_{\mathbb{B}}$  and  $s$  denotes the position of a point of the tail rotor in a rotor-fixed reference frame. In this case, it holds that

$$\frac{d}{dt} [p + R(b_t + R_t s)] = \dot{p} + \dot{R}(b_t + R_t s) + R \dot{R}_t s = \dot{p} + R \xi b_t + R(\xi + \xi_t) R_t s, \quad (3.31)$$

where  $\dot{R}_t = \xi_t R_t$ . The angular velocity matrix  $\xi_t \in \mathfrak{so}(3)$  of the principal rotor is controlled by the pilot and is hence to be held as a known quantity. Since the instantaneous axis of rotation of the tail rotor is fixed and coincides to the  $-y$  axis, the angular matrix  $\xi_t$  takes the explicit expression

$$\xi_t := -\Omega_t \xi_y = \begin{bmatrix} 0 & 0 & -\Omega_t \\ 0 & 0 & 0 \\ \Omega_t & 0 & 0 \end{bmatrix}, \quad (3.32)$$

where  $\Omega_t$  denotes the instantaneous rotation speed of the tail rotor.

The kinetic energy of the tail rotor  $\mathcal{T}$  in the earth frame  $\mathcal{F}_{\mathbb{E}}$  has an expression which is derived in a similar manner to (3.26) and may be written as

$$\begin{aligned} \ell_{\mathcal{T}} = & \frac{1}{2} M_{\mathcal{T}} \|\dot{p}\|^2 + \frac{1}{2} M_{\mathcal{T}} \text{tr}(\xi b_t b_t^{\top} \xi^{\top}) + \frac{1}{2} \text{tr}((\xi + \xi_t) R_t \hat{J}_{\mathcal{T}} R_t^{\top} (\xi + \xi_t)^{\top}) + \\ & M_{\mathcal{T}} \text{tr}(\dot{p} b_t^{\top} \xi^{\top} R^{\top}) + M_{\mathcal{T}} \text{tr}(\dot{p} c_{\mathcal{T}}^{\top} R_t^{\top} (\xi + \xi_t) R^{\top}) + M_{\mathcal{T}} \text{tr}(\xi b_t c_{\mathcal{T}}^{\top} R_t^{\top} (\xi + \xi_t)^{\top}) \end{aligned} \quad (3.33)$$

where

$$M_{\mathcal{T}} := \int_{\mathcal{T}} dm > 0, \quad \hat{J}_{\mathcal{T}} := \int_{\mathcal{T}} s s^{\top} dm \in \mathbb{R}^{3 \times 3} \quad \text{and} \quad c_{\mathcal{T}} := \frac{1}{M_{\mathcal{T}}} \int_{\mathcal{T}} s dm \in \mathbb{R}^3. \quad (3.34)$$



In order to simplify the expression (3.33), we may assume that the tail rotor is perfectly symmetric about its own centre of mass  $c_{\mathcal{T}}$ , which implies that  $c_{\mathcal{T}} = 0$ . Moreover, we may assume that the tail rotor may be schematized as a full disk of mass  $M_{\mathcal{T}}$  and radius  $l_{\mathcal{T}}$  laying over the  $x - z$  plane spinning around the  $y$ -axis, namely that

$$J_{\mathcal{T}} = \begin{bmatrix} j_{\mathcal{T}} & 0 & 0 \\ 0 & 2j_{\mathcal{T}} & 0 \\ 0 & 0 & j_{\mathcal{T}} \end{bmatrix}, \text{ that is, } \hat{J}_{\mathcal{T}} = j_{\mathcal{T}} \text{diag}(1, 0, 1), \quad (3.35)$$

by Lemma 3.2, with  $j_{\mathcal{T}} := \frac{1}{4}M_{\mathcal{T}}l_{\mathcal{T}}^2$ . Since

$$R_t = \begin{bmatrix} \cos \theta_t & 0 & -\sin \theta_t \\ 0 & 1 & 0 \\ \sin \theta_t & 0 & \cos \theta_t \end{bmatrix}, \quad (3.36)$$

direct calculations show that  $R_t \hat{J}_{\mathcal{T}} R_t^{\top} = \hat{J}_{\mathcal{T}}$ . Therefore, the kinetic energy of the tail rotor is given by

$$\ell_{\mathcal{T}} = \frac{1}{2}M_{\mathcal{T}}\|\dot{p}\|^2 + \frac{1}{2}M_{\mathcal{T}}\text{tr}(\xi b_t b_t^{\top} \xi^{\top}) + \frac{1}{2}\text{tr}((\xi + \xi_t)\hat{J}_{\mathcal{T}}(\xi + \xi_t)^{\top}) + M_{\mathcal{T}}\text{tr}(\dot{p} b_t^{\top} \xi^{\top} R_t^{\top}) \quad (3.37)$$

Rearranging terms shows that the kinetic energy of the tail rotor may be written equivalently as

$$\ell_{\mathcal{T}} = \frac{1}{2}M_{\mathcal{T}}\|\dot{p} + R\xi b_t\|^2 + \frac{1}{2}\text{tr}((\xi + \xi_t)\hat{J}_{\mathcal{T}}(\xi + \xi_t)^{\top}), \quad (3.38)$$

where the first term represents the translational kinetic energy of the centre of mass of the tail rotor and the second term represents the rotational kinetic energy of the tail rotor, both expressed in the reference frame  $\mathcal{F}_E$ .

**Potential energy of a helicopter:** The potential energy associated to the helicopter is  $(M_{\mathcal{B}} + M_{\mathcal{R}} + M_{\mathcal{T}})\bar{g}e_z^{\top}p$ , where the scalar  $\bar{g}$  denotes the gravitational acceleration.

**Lagrangian of a helicopter:** The Lagrangian function associated to a helicopter model is hence obtained by gathering the kinetic energies (3.23), (3.29), (3.37) and the potential energy as

$$\begin{aligned} \ell_{\mathcal{H}} &:= \ell_{\mathcal{B}} + \ell_{\mathcal{R}} + \ell_{\mathcal{T}} - (M_{\mathcal{B}} + M_{\mathcal{R}} + M_{\mathcal{T}})\bar{g}e_z^{\top}p \\ &= \frac{1}{2}M_{\mathcal{B}}\|\dot{p}\|^2 + \frac{1}{2}\text{tr}(\xi \hat{J}_{\mathcal{B}} \xi^{\top}) + M_{\mathcal{B}}\text{tr}(\dot{p} c_{\mathcal{B}}^{\top} \xi^{\top} R^{\top}) + \\ &\quad \frac{1}{2}M_{\mathcal{R}}\|\dot{p}\|^2 + \frac{1}{2}M_{\mathcal{R}}\text{tr}(\xi b_m b_m^{\top} \xi^{\top}) + \frac{1}{2}\text{tr}((\xi + \xi_m)\hat{J}_{\mathcal{R}}(\xi + \xi_m)^{\top}) + M_{\mathcal{R}}\text{tr}(\dot{p} b_m^{\top} \xi^{\top} R^{\top}) + \\ &\quad \frac{1}{2}M_{\mathcal{T}}\|\dot{p}\|^2 + \frac{1}{2}M_{\mathcal{T}}\text{tr}(\xi b_t b_t^{\top} \xi^{\top}) + \frac{1}{2}\text{tr}((\xi + \xi_t)\hat{J}_{\mathcal{T}}(\xi + \xi_t)^{\top}) + M_{\mathcal{T}}\text{tr}(\dot{p} b_t^{\top} \xi^{\top} R^{\top}) - \\ &\quad (M_{\mathcal{B}} + M_{\mathcal{R}} + M_{\mathcal{T}})\bar{g}e_z^{\top}p. \end{aligned}$$

The expression of the Lagrangian  $\ell_{\mathcal{H}}$  contains several similar terms and may be rewritten compactly as

$$\begin{aligned} \ell_{\mathcal{H}} &= \frac{1}{2}M_{\mathcal{H}}\|\dot{p}\|^2 + \frac{1}{2}\text{tr}(\xi \hat{J}_{\mathcal{H}} \xi^{\top}) + M_{\mathcal{H}}\text{tr}(\dot{p} c_{\mathcal{H}}^{\top} \xi^{\top} R^{\top}) + \\ &\quad \frac{1}{2}\text{tr}((\xi + \xi_m)\hat{J}_{\mathcal{R}}(\xi + \xi_m)^{\top}) + \frac{1}{2}\text{tr}((\xi + \xi_t)\hat{J}_{\mathcal{T}}(\xi + \xi_t)^{\top}) - M_{\mathcal{H}}\bar{g}e_z^{\top}p. \end{aligned} \quad (3.39)$$

where

$$M_{\mathcal{H}} := M_{\mathcal{B}} + M_{\mathcal{R}} + M_{\mathcal{T}}, \quad \hat{J}_{\mathcal{H}} := \hat{J}_{\mathcal{B}} + M_{\mathcal{R}}b_m b_m^{\top} + M_{\mathcal{T}}b_t b_t^{\top}, \quad c_{\mathcal{H}} := \frac{1}{M_{\mathcal{H}}}(M_{\mathcal{B}}c_{\mathcal{B}} + M_{\mathcal{R}}b_m + M_{\mathcal{T}}b_t). \quad (3.40)$$

Since the origin of the body-fixed reference frame was taken at the centre of gravity of the helicopter, it holds that  $c_{\mathcal{H}} = 0$ , therefore the helicopter's Lagrangian takes the final expression

$$\ell_{\mathcal{H}}(\dot{p}, \xi, p) = \frac{1}{2}M_{\mathcal{H}}\|\dot{p}\|^2 - \frac{1}{2}\text{tr}(\hat{J}_{\mathcal{H}}\xi^2) - \frac{1}{2}\text{tr}(\hat{J}_{\mathcal{R}}(\xi + \xi_{\text{m}})^2) - \frac{1}{2}\text{tr}(\hat{J}_{\mathcal{T}}(\xi + \xi_{\text{t}})^2) - M_{\mathcal{H}}\frac{(\mathbb{R}\bar{1})}{2}p$$

where we have used the Lie-algebra property that  $\xi^{\top} = -\xi$  and the cyclic permutation property of the trace operator. The Lagrangian (3.41) is a function of the variables  $\dot{p}$ ,  $\xi$  and  $p$ .

### 3.3 Rotational component of motion

The rotational component of motion, which governs the evolution of the Lie-algebra variable  $\xi$ , is described by the Euler-Poincaré equations (3.1) applied to the Lagrangian function (3.41) and to the rotors-generated mechanical torque (3.7).

As a first step, it is necessary to compute the fiber derivative of the Lagrangian  $\ell_{\mathcal{H}}$ . The Jacobian of the Lagrangian at a point  $\xi$  may be computed easily by the property:

$$\ell_{\mathcal{H}}(\xi + \Delta\xi) - \ell_{\mathcal{H}}(\xi) = \text{tr}(\Delta\xi^{\top} \mathbf{J}_{\xi} \ell_{\mathcal{H}}) + \text{higher-order terms in } \Delta\xi, \quad (3.42)$$

where  $\Delta\xi$  denotes an arbitrary perturbation. It is essential to recall that, while evaluating the jacobian, the matrix  $\xi$  is to be considered as unconstrained (namely, not an element of  $\mathfrak{g}$ ). Straightforward calculations give

$$\mathbf{J}_{\xi} \ell_{\mathcal{H}} = -\frac{1}{2} \left( \{\xi, \hat{J}_{\mathcal{H}}\}^{\top} + \{\xi + \xi_{\text{m}}, \hat{J}_{\mathcal{R}}\}^{\top} + \{\xi + \xi_{\text{t}}, \hat{J}_{\mathcal{T}}\}^{\top} \right). \quad (3.43)$$

Plugging the above expression into the relation (3.4) and recalling that the inertia tensors are symmetric matrices, one gets the angular momentum

$$\frac{\partial \ell_{\mathcal{H}}}{\partial \xi} = \{ \{ \mathbf{J}_{\xi} \ell_{\mathcal{H}} \} \} = \frac{1}{2} \left( \{\xi, \hat{J}_{\mathcal{H}}\} + \{\xi + \xi_{\text{m}}, \hat{J}_{\mathcal{R}}\} + \{\xi + \xi_{\text{t}}, \hat{J}_{\mathcal{T}}\} \right). \quad (3.44)$$

It pays to recall that the anti-commutator is a bilinear form, hence, upon defining

$$\hat{J}_{\mathcal{H}}^{\star} := \hat{J}_{\mathcal{H}} + \hat{J}_{\mathcal{R}} + \hat{J}_{\mathcal{T}}, \quad (3.45)$$

the angular momentum (3.44) may be simplified to

$$\mu := \frac{\partial \ell_{\mathcal{H}}}{\partial \xi} = \frac{1}{2} \left( \{\xi, \hat{J}_{\mathcal{H}}^{\star}\} + \{\xi_{\text{m}}, \hat{J}_{\mathcal{R}}\} + \{\xi_{\text{t}}, \hat{J}_{\mathcal{T}}\} \right). \quad (3.46)$$

The angular momentum  $\mu$  represents the ‘quantity of rotational motion’ of the helicopter as it is proportional to the inertia and to the rotational speed of its components. The time-derivative of the angular momentum may be rewritten as

$$\dot{\mu} = \frac{d}{dt} \frac{\partial \ell_{\mathcal{H}}}{\partial \xi} = \frac{1}{2} \left( \{\dot{\xi}, \hat{J}_{\mathcal{H}}^{\star}\} + \{\dot{\xi}_{\text{m}}, \hat{J}_{\mathcal{R}}\} + \{\dot{\xi}_{\text{t}}, \hat{J}_{\mathcal{T}}\} \right), \quad (3.47)$$

and direct calculations lead to

$$-\text{ad}_{\xi} \left( \frac{\partial \ell_{\mathcal{H}}}{\partial \xi} \right) = \left[ \frac{\partial \ell_{\mathcal{H}}}{\partial \xi}, \xi \right] = \frac{1}{2} [\hat{J}_{\mathcal{H}}^{\star}, \xi^2] + \frac{1}{2} \left[ \{\xi_{\text{m}}, \hat{J}_{\mathcal{R}}\} + \{\xi_{\text{t}}, \hat{J}_{\mathcal{T}}\}, \xi \right]. \quad (3.48)$$

The term  $\dot{\mu}$  represents the rate of change of the angular momentum that, by the angular momentum theorem, is equal to the total torque acting on the helicopter.

To take into account energy dissipation due to friction between the helicopter and the air molecules during rotation of the helicopter along the vertical direction, that tends to brake the motion of the helicopter, the equation governing the rotational motion may be completed by introducing a non-conservative force proportional to the helicopter rotation speed along the  $z$ -axis. The resulting Euler-Poincaré equation for the helicopter model reads

$$\{\dot{\xi}, \hat{J}_{\mathcal{H}}^*\} = [\hat{J}_{\mathcal{H}}^*, \xi^2] + \left[ \{\xi_{\text{m}}, \hat{J}_{\mathcal{R}}\} + \{\xi_{\text{t}}, \hat{J}_{\mathcal{T}}\}, \xi \right] - \{\dot{\xi}_{\text{m}}, \hat{J}_{\mathcal{R}}\} - \{\dot{\xi}_{\text{t}}, \hat{J}_{\mathcal{T}}\} + 2\tau - \beta_{\text{r}} \langle \xi, \xi_z \rangle \xi_z. \quad (3.49)$$

where  $\beta_{\text{r}} \geq 0$  is a coefficient that quantifies the braking action of the air around the helicopter during fast yawing.

### 3.4 Translational component of motion

The translation component of motion obeys the Euler-Poincaré equation (2.12) written in the inertial (earth) reference frame  $\mathcal{F}_{\text{E}}$ . In this case, the non-conservative force field is given by the total thrust  $\varphi_{\text{m}} + \varphi_{\text{t}}$  rotated of a quantity  $R$  to express it in the earth frame  $\mathcal{F}_{\text{E}}$ , therefore, the Euler-Poincaré equation reads:

$$\frac{d}{dt} \frac{\partial \ell_{\mathcal{H}}}{\partial \dot{p}} = \frac{\partial \ell_{\mathcal{H}}}{\partial p} + R(\varphi_{\text{m}} + \varphi_{\text{t}}). \quad (3.50)$$

Notice that

$$\frac{d}{dt} \frac{\partial \ell_{\mathcal{H}}}{\partial \dot{p}} = M_{\mathcal{H}} \ddot{p}, \quad \frac{\partial \ell_{\mathcal{H}}}{\partial p} = -M_{\mathcal{H}} \bar{g} e_z. \quad (3.51)$$

To take into account energy dissipation due to friction between the helicopter and the air molecules, that tends to brake the motion of the helicopter, the equation governing the translation motion may be completed by introducing a non-conservative force proportional to the helicopter speed. Ultimately, the equation which describes the translational motion of a helicopter may be written as follows:

$$M_{\mathcal{H}} \ddot{p} = R(\varphi_{\text{m}} + \varphi_{\text{t}}) - M_{\mathcal{H}} \bar{g} e_z - B \dot{p}, \quad (3.52)$$

where  $B := \text{diag}(\beta_{\text{h}}, 0, \beta_{\text{v}})$ . The non-negative coefficients  $\beta_{\text{h}}$  and  $\beta_{\text{v}}$  quantify the braking action on the helicopter which is more pronounced along the vertical direction than horizontally, due to the helicopter's shape.

Focusing on the equation (3.52) it is possible to see that when the helicopter is horizontal, namely  $R = I_3$ , the tail rotor influences the horizontal component of the second derivative of the position  $p$ . The tail rotor term when the helicopter is tilted ( $R \neq I_3$ ) causes an additional difficulty in controlling the position of the helicopter.

### 3.5 Explicit state-space form of the equations of motion

In order to write the equations of motion in an explicit form, we start off with a few important simplifications.

The terms related to the principal rotors may be rewritten explicitly as follows. The term  $\{\Omega_m \xi_z, \hat{J}_R\} = j_R \Omega_m \{\xi_z, \text{diag}(1, 1, 0)\} = 2j_R \Omega_m \xi_z$ . Likewise, the term  $\{\dot{\Omega}_m \xi_z, \hat{J}_R\} = 2j_R \dot{\Omega}_m \xi_z$ .

The terms related to the tail rotors may be rewritten explicitly by noticing that the term  $\{-\Omega_t \xi_y, \hat{J}_T\} = -j_T \Omega_t \{\xi_y, \text{diag}(1, 0, 1)\} = -2j_T \Omega_t \xi_y$ . Likewise, the term  $\{-\dot{\Omega}_t \xi_y, \hat{J}_T\} = -2j_T \dot{\Omega}_t \xi_y$ .

The constant  $\hat{J}_H^* = \hat{J}_B + M_R b_m b_m^\top + M_T b_t b_t^\top + \hat{J}_R + \hat{J}_T$ . Notice that  $b_m b_m^\top = D_m^2 \text{diag}(0, 0, 1)$  and  $b_t b_t^\top = D_t^2 \text{diag}(1, 0, 0)$ . In addition, recall that the reference frame  $\mathcal{F}_B$  has been chosen with the orthogonal axes coincident with the principal axes of inertia of the fuselage itself, hence the tensor  $\hat{J}_B$  is diagonal. As a consequence, the total helicopter's non-standard inertia tensor is diagonal, namely  $\hat{J}_H^* = \text{diag}(j_x, j_y, j_z)$ .

As a last observation, the quantity  $\{\dot{\xi}, \hat{J}_H^*\}$  may be written equivalently as  $S \dot{\xi} S$ , where  $S := \text{diag}(s_x, s_y, s_z)$ , with

$$s_x := \sqrt{\frac{(j_x + j_y)(j_x + j_z)}{j_y + j_z}}, \quad s_y := \sqrt{\frac{(j_y + j_x)(j_y + j_z)}{j_x + j_z}}, \quad s_z := \sqrt{\frac{(j_z + j_x)(j_z + j_y)}{j_x + j_y}}. \quad (3.53)$$

**Explicit equations of motion:** The equation of motion of the helicopter model taken into consideration in the present paper may be written explicitly as

$$\begin{cases} \dot{R} = R\xi, \\ \dot{\xi} = S^{-1} \left( [\hat{J}_H^*, \xi^2] + 2[j_R \dot{\Omega}_m \xi_z - j_T \dot{\Omega}_t \xi_y, \xi] - 2j_R \dot{\Omega}_m \xi_z + 2j_T \dot{\Omega}_t \xi_y + 2\tau - \beta_r \langle \xi, \xi_z \rangle \xi_z \right) S^{-1}, \\ \tau := \frac{1}{2} D_m u_m \sin \alpha_r \xi_x + \frac{1}{2} D_m u_m \sin \alpha_p \cos \alpha_r \xi_y + \frac{1}{2} (D_t u_t - \gamma u_m) \xi_z, \\ \ddot{p} = \frac{1}{M_H} R \varphi - \bar{g} e_z - \frac{1}{M_H} B \dot{p}, \\ \varphi := \begin{bmatrix} \frac{1}{2} u_m \sin \alpha_p \cos \alpha_r \\ -\frac{1}{2} u_m \sin \alpha_r - \frac{1}{2} u_t \\ \frac{1}{2} u_m \cos \alpha_p \cos \alpha_r \end{bmatrix}. \end{cases} \quad (3.54)$$

It is interesting to consider a few special cases of motion and how the model (3.54) would simplify.

**Free fall:** Let us assume that both rotors are blocked ( $\xi_m = \xi_t = 0$ ) and that they are isolated from the pilot control ( $u_m = u_t = 0$ ). In this case, the external torque  $\tau$  (3.7) is null. The rotational component of motion is hence described by  $\{\dot{\xi}, \hat{J}_B + M_R b_m b_m^\top + M_T b_t b_t^\top + \hat{J}_R + \hat{J}_T\} = [\hat{J}_B + M_R b_m b_m^\top + M_T b_t b_t^\top + \hat{J}_R + \hat{J}_T, \xi^2]$ , which represents the classical equation of a rigid body rotating freely in space under inertial forces (generally known as Euler's equation of a free rigid body).

**Constant rotor speed and negligible rotational inertia:** Assuming constant rotation speed for the principal and the tail rotors (namely,  $\dot{\xi}_m = \dot{\xi}_t = 0$ ) and assuming that the angular momentum of the tail rotor and of the principal rotor are negligible with respect to the angular momentum of the helicopter, we obtain the simplified model  $\frac{1}{2}\{\dot{\xi}, \hat{J}_B + M_{\mathcal{R}}b_m b_m^\top + M_{\mathcal{T}}b_t b_t^\top\} = \frac{1}{2}[\hat{J}_B + M_{\mathcal{R}}b_m b_m^\top + M_{\mathcal{T}}b_t b_t^\top, \xi^2] + \tau$ , that is the helicopter model studied in [2].

**Hovering:** Using as reference  $\mathcal{F}_E$ , hovering happens when the weight  $M_{\mathcal{H}}\bar{g}$  balances the  $z$ -component of the thrust. In this situation the helicopter may only translate sideways in the  $x - y$  plane. Recalling that

$$\varphi = \varphi_m + \varphi_t = \begin{bmatrix} \frac{1}{2}u_m \sin \alpha_p \cos \alpha_r \\ -\frac{1}{2}u_m \sin \alpha_r - \frac{1}{2}u_t \\ \frac{1}{2}u_m \cos \alpha_p \cos \alpha_r \end{bmatrix},$$

defining:

$$\varphi_w := e_z^\top \begin{bmatrix} 0 \\ 0 \\ -M_{\mathcal{H}}\bar{g} \end{bmatrix} \quad \text{and} \quad \varphi_z := e_z^\top (R\varphi)e_z, \quad (3.55)$$

the hovering condition reads

$$\varphi_z + \varphi_w = 0. \quad (3.56)$$

Supposing the helicopter in horizontal position with  $\mathcal{F}_B$  and  $\mathcal{F}_E$ 's  $z$ -axes overlapped, the equation (3.56) becomes  $2M_{\mathcal{H}}\bar{g} = u_m$ . Detailing the main rotor thrust formula (3.12), it could be read as  $4M_{\mathcal{H}}\bar{g} = C_u \rho \pi l_R^4 \Omega_m^2 \sin \alpha_c$ . Hence, the collective angle needed resulting from the hovering condition takes the form

$$\alpha_{c,\text{hover}} = \arcsin \left( \frac{4M_{\mathcal{H}}\bar{g}}{C_u \rho \pi l_R^4 \Omega_m^2} \right). \quad (3.57)$$

Either changing of the angle  $\alpha_p$  or  $\alpha_r$  causes a decrease of the  $z$ -axis thrust value, so every time that the *cyclic control* is used the helicopter tends to fall. Taking into account that the falling condition could happen when the driver sets up the landing, we clearly need to prevent it forcing the hover. The equation below gives us the value of the right collective angle with respect to  $\alpha_r$  and  $\alpha_p$  in order to do not fall:

$$\alpha_{c,\text{hover}} = \arcsin \left( \frac{2M_{\mathcal{H}}\bar{g}}{u_m \sin(\alpha_p) \sin(\alpha_r)} \right). \quad (3.58)$$

The maximum linear velocity along the  $x$ -axis could be reached through two hypothesis: the first is the hovering condition, in order to balance the weight force and not to decrease the helicopter height, and the second is splitting the remainder part of the thrust in a component purely directed along the  $x$ -axis, namely  $\alpha_r = 0$ . Clearly from (3.56) the formula to find this particular pitch angle is:

$$\alpha_{p,\text{maxSpeed}} = \arccos \left( 2 \frac{M_{\mathcal{H}}\bar{g}}{\bar{u}_m} \right), \quad (3.59)$$

where  $\bar{u}_m$  is a known value of the thrust greater than the weight force of the helicopter.

*Remark:* As the *collective control* changes the torque exerted by the main rotor, this procedure implies a number of concurrent actions. In fact, consider the driver wants to

change the attitude using the *cyclic control* and needs the hovering condition: the *cyclic control* causes the need to boost the thrust by using the *collective control*, and the *collective control* causes an increase of the torque and hence a yaw effect which requires the *pedals control* to be managed.

**No yawing:** The condition of no yawing is achieved when  $\langle \xi, \xi_z \rangle$  stays constant to 0. Namely, the helicopter does not turn around the  $z$ -axis. In this case the friction due to rotation,  $\beta_r \langle \xi, \xi_z \rangle$ , is 0. Considering  $\xi = 0$  at some time, it is necessary to have the first derivative of the angular velocity equal to zero, hence  $\langle \dot{\xi}, \xi_z \rangle = 0$ . From (3.54), it follows that

$$S^{-1} (-2j_{\mathcal{R}} \dot{\Omega}_m \xi_z + (D_t u_t - \gamma u_m) \xi_z) S^{-1} = 0. \quad (3.60)$$

As it was already underlined while discussing equations (3.9), in the case of constant main rotor speed  $\Omega_m$ , the condition (3.60) will become  $S^{-1} ((D_t u_t - \gamma u_m) \xi_z) S^{-1} = 0$  that could be reduced to  $D_t u_t = \gamma u_m$ .

**No drifting:** The tail thrust causes the helicopter to drift along the  $y$ -axis. This side effect may be compensated by choosing appropriately the angle of attack  $\alpha_r$  of the helicopter. The equilibrium along the  $y$ -axis is reached when  $\varphi^\top e_y = 0$  (where  $e_y := [0 \ 1 \ 0]^\top$ ). Since  $\varphi^\top e_y = -\frac{1}{2} u_m \sin \alpha_r - \frac{1}{2} u_t$  in order not to have longitudinal forces the roll angle has to be set as:

$$\alpha_{r, \text{nodrift}} = -\arcsin \left( \frac{u_t}{u_m} \right). \quad (3.61)$$

With this value of the angle of attack, the net drift force along the  $y$ -axis will drop to zero, meaning that no acceleration along the  $y$ -axis will be detected, although any pre-existing motions along the  $y$ -axis will not cease. Moreover, setting the angle of attack  $\alpha_r$  to this value will cause the fuselage to roll.

## Numerical aspects

The system of differential equations (3.54) has to be discretized in order to be implemented in a calculator.

An ordinary differential equation, in which the initial value is known, could be resolved numerically using the forward Euler method *fEul*. The first derivative of a function could be approximated numerically as:

$$\dot{f}_{k-1} = \frac{f_k - f_{k-1}}{h} \quad (4.1)$$

whereas the second derivative of a function could be approximated numerically iterating the *fEul* method as follows

$$\ddot{f}_{k-1} = \frac{\dot{f}_k - \dot{f}_{k-1}}{h} \quad (4.2)$$

where  $k \geq 1$ , and  $h$  represents the step of resolution of the numerical method. Developing the equations (4.1) and (4.2), the second derivative equation of a function may be approximated by  $\ddot{f}_{k-2} = \frac{f_k - 2f_{k-1} + f_{k-2}}{h^2}$ .

Using the result in equation (3.54), it is possible to end up with the equation to find the position numerically:

$$\frac{1}{M_{\mathcal{H}}} R_{k-2} \varphi_{k-2} - \bar{g} e_z - \frac{1}{M_{\mathcal{H}}} B \left( \frac{p_{k-1} - p_{k-2}}{h} \right) = \frac{p_k - 2p_{k-1} + p_{k-2}}{h^2},$$

which becomes:

$$p_k = \frac{h^2}{M_{\mathcal{H}}} R_{k-2} \varphi_{k-2} - h^2 \bar{g} e_z - \frac{h}{M_{\mathcal{H}}} B (p_{k-1} - p_{k-2}) + 2p_{k-1} - p_{k-2}. \quad (4.3)$$

The equation  $\dot{R} = R\xi$  describes the first-order derivative of the helicopter's attitude. The attitude  $R$  belongs to  $\text{SO}(3)$  and in manifolds it is not possible to perform subtraction and, as a consequence, use directly the *fEul* method. In this case, it is necessary to use exponential map, thus:

$$R_k = \exp_{R_{k-1}}(h R_{k-1} \xi_{k-1}). \quad (4.4)$$

Using the expression of exponential map tailored for  $\text{SO}(3)$  the final result is

$$R_k = R_{k-1} \text{Exp}(h \xi_{k-1}), \quad (4.5)$$

where 'Exp' is the matrix exponential. Continuing to process numerically the equations from (3.54), we managed to process the angular acceleration equation, which is

$$\begin{aligned} \dot{\xi} = S^{-1} & \left( [\hat{J}_{\mathcal{H}}^*, \xi^2] + 2[j_{\mathcal{R}}\dot{\Omega}_m \xi_z - j_{\mathcal{T}}\dot{\Omega}_t \xi_y, \xi] \right. \\ & \left. - 2j_{\mathcal{R}}\dot{\Omega}_m \xi_z + 2j_{\mathcal{T}}\dot{\Omega}_t \xi_y + 2\tau - \beta_r \langle \xi, \xi_z \rangle \xi_z \right) S^{-1}. \end{aligned} \quad (4.6)$$

Since the equation describes two members which belong to the same tangent space  $\mathfrak{g}$ , we could use the classical Euler's method:  $\xi_k = \xi_{k-1} + h \dot{\xi}_{k-1}$ . In particular,  $\dot{\xi}_{k-1}$  represents the angular acceleration at the step  $k - 1$ . At the end of the day, the final numerical solution reads:

$$\begin{aligned} \dot{\xi}_{k-1} = S^{-1} & \left( [\hat{J}_{\mathcal{H}}^*, \xi_{k-1}^2] + 2[j_{\mathcal{R}}\dot{\Omega}_{m,k-1} \xi_z - j_{\mathcal{T}}\dot{\Omega}_{t,k-1} \xi_y, \xi_{k-1}] \right. \\ & \left. - 2j_{\mathcal{R}}\dot{\Omega}_{m,k-1} \xi_z + 2j_{\mathcal{T}}\dot{\Omega}_{t,k-1} \xi_y + 2\tau_{k-1} - \beta_r \langle \xi_{k-1}, \xi_z \rangle \xi_z \right) S^{-1}. \end{aligned} \quad (4.7)$$



# Helicopter type and value of the parameters

To implement the mathematical model studied, it is necessary to choose a specific helicopter model and gather values from certification sheets and data-sheets. The model chosen for this study is the EC135 P2+, also known as H135 P2+ manufactured from Airbus Helicopter, leader in the field of emergency medical services.

The data have been gathered from the manufacturer's flight manual [3], and other manuals [5, 1, 6, 22, 9, 8, 7, 4].

The EC135 P2+ helicopter is equipped with a 4-blades bearingless main rotor and a 10-blades tail rotor.

## 5.1 Main rotor and tail rotor characteristics

The main characteristics of the tail and the main rotor are collected in Table 5.1.

|         | Weight             | Speed 100% | Collect. Angle       | Cyclic Angle    |               |
|---------|--------------------|------------|----------------------|-----------------|---------------|
|         | [kg]               | [RPM]      | min-max [deg]        | longitud. [deg] | lateral [deg] |
| M.rotor | 277.2 <sup>§</sup> | 395        | 11 ÷ 31 <sup>¶</sup> | -21.8 ÷ 21.8    | -15 ÷ 15      |
| T.rotor | 8.2                | 3584       | -16.8 ÷ 34.2         |                 |               |

Table 5.1: Tail rotor collective angle range, tail rotor weight, speed main rotor ([1] page 303, 254 and 157), tail rotor speed ([4] page 3), cycling angle page (11 in [5]).

<sup>§</sup>The main rotor weight is the result of the addition of various parts which compose the entire main rotor. These values have been taken from [6], page 3, which is the technical data-sheet of the helicopter AS350B3 also known as H125, that is the lower level helicopter by the same manufacturer. The values taken have not been modified because the model is supposed to be similar. The final weight is calculated by the sum of: anti-vibration device (28.4kg), main rotor mast (55.7kg), rotor hub (57.5kg) and 4 blades ( $4 \cdot 33.9 = 135,6\text{kg}$ )

<sup>¶</sup>As stated in [22] page 57 the value of the collective angle could vary in the range [-5,15] degrees and the negative angle could be necessary to achieve zero lift if blades have a built-in axial

## 5.2 Dimensions and center of mass

The Figure 5.1 shows the principal dimension values. The relevant values have been collected in Table 5.2

|                       | Dimensions |          |          | Weight               |
|-----------------------|------------|----------|----------|----------------------|
|                       | [m]        |          |          | [kg]                 |
| Main rotor blade      | 5.1        |          |          | 33.9 <sup>  </sup>   |
| Tail rotor blade      | 0.5        |          |          | /                    |
| <i>reference axis</i> | <i>x</i>   | <i>y</i> | <i>z</i> |                      |
| Fuselage              | 5.87       | 1.56     | 2.20     | 1134.6 <sup>**</sup> |

Table 5.2: Dimensions are taken from [3], page 7, and the weight of the main rotor blade from [6], page 3.

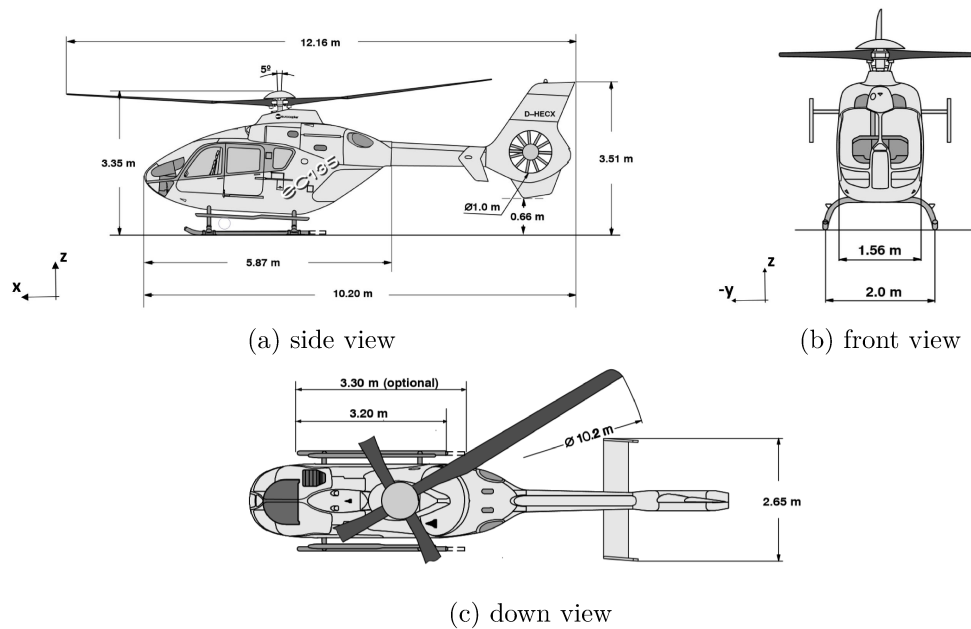


Figure 5.1: Dimensions of the EC135 P2+, the picture is taken from [3].

To calculate the centre of mass of the helicopter it is necessary to split the helicopter's structure in three major parts, as done in the study of the model:

### 1. The fuselage or body

*twist.* From reference [1], page 200, we know that the EC135 P2+ helicopter has a positive twist of 16 degrees in the region where the pitch control cuff joins the airfoil section. This provides the airfoil section with a corresponding preset pitch angle. Using the equation (3.12) the collective angles range becomes [11, 31] degrees, respectively the minimum angle and the maximum angle to change the thrust generated.

<sup>||</sup>The value of the height is not mentioned in any of the sources found, therefore it has been calculated from the technical design.

<sup>\*\*</sup>The fuselage weight has been found as the weight of the empty helicopter, that is 1420 kg, removing the weight of the main rotor and the tail rotor. The helicopter weight value is taken from [5], page 2.

2. The main rotor
3. The tail rotor

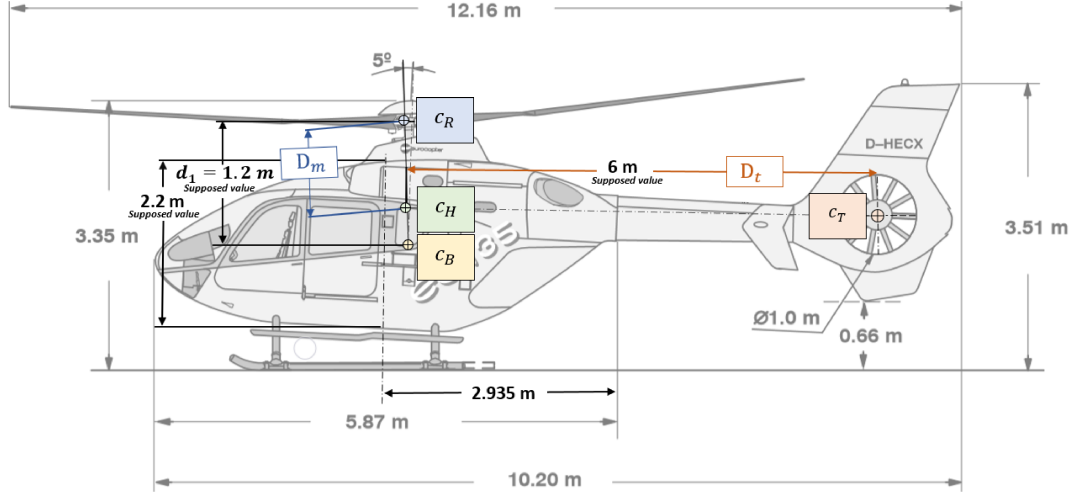


Figure 5.2: Values used to calculate the centre of mass. Picture taken from [3], page 7.

It is necessary to make some assumptions to calculate the centre of mass of the helicopter and to find the value  $D_m$  and  $D_t$ , all these assumptions refer to the Figure 5.2. It is assumed that  $c_B$  lies in the axis passing through the rotor and perpendicular to the base. Furthermore, suppose  $c_R$  located in the axis 5 degrees tilted from the vertical one. In addition, we may think of the main rotor and the body as two objects composing the system *Body – MainRotor* ( $B, R$ ), and the reference system in this case with the origin located in the point  $c_B$  and one axis which matches the axis 5 degrees tilted toward the point  $c_R$ . We can find  $c_{B,R}$  by the equation

$$c_{B,R} = \frac{Weight_{MainRotor}}{Weight_{MainRotor} + Weight_{Body}} \cdot d_1. \quad (5.1)$$

Now, assuming  $d_1 = 1.2$  m as the distance from  $c_B$  and  $c_R$ , the above equation gives

$$c_{B,R} = \frac{277.2}{277.2 + 1134.6} \cdot 1.2 \cong 0.235614 \text{ meters} \quad (5.2)$$

Moreover, it is supposed that the contribution of the point  $c_T$  could be disregarded since the weight of the tail rotor is negligible compared to the fuselage weight and the main rotor weight. Therefore, the tail rotor does not contribute to the calculations of the helicopter centre of mass, hence it results  $c_{B,R} \cong c_H$ . The value of  $D_t$  has been supposed using the data-sheets, and  $D_m$ , that is the distance from the centre of gravity of the helicopter and the main rotor, is  $D_m = d_1 - c_H \cong 0.964386$  m.

## 5.3 Engines and gear box

The EC135 P2+ helicopter type is equipped with two PW206B2 engines from Pratt and Whitney Canada Corp. To start engines there are two possibilities: manual control or automatic control. The manual control is not certificated and normally deactivated. The automatic control is managed by the FADEC (Full Authority Digital Engine Control) that controls the starting procedure, the fuel flow and the RPMs automatically. At the start of the engines the FADEC turns on the engines one by one until the RPMs reach the value of 98% ([1] page 437). When either the *collective control* or the flight switch are changed the FADEC will increase the RPMs to 100% and the flight mode will start. When the altitude is higher than 4000ft the speed is automatically increased to 104%, because of the air density  $\rho$  decrease. Moreover, to avoid loss of thrust when the collective angle is changed in the main rotor (pitch) or in the tail rotor (yaw) the FADEC fixes the engine power to maintain the desired speed. The characteristics of the engines are summarized in Table 5.3:

| Engine mode           | Power          | max. Torque    |
|-----------------------|----------------|----------------|
|                       | [ kW ]         | [ N · m ]      |
| AEO TOP (max. 5 min.) | $2 \times 333$ | $2 \times 519$ |
| AEO MCP               | $2 \times 321$ | $2 \times 500$ |
| OEI (max. 30s.)       | 547            | 851            |
| OEI (max. 2min.)      | 534            | 831            |
| OEI MCP               | 404            | 629            |

Table 5.3: Values are taken from [7], page 8 and 12. The helicopter state AEO means all engine operatives, whereas the state OEI is the short for one engine inoperative. Usually, the second state occurs when there is a problem in one engine. Typically, two possible working mode could be selected TOP (take-off power), which has a time limit constrain, and MCP (maximum continuous power).

The gear box is a complex part that transmits power, usually reducing angular velocity and increasing torque. Both helicopter engines drive the gear box that, in turn, drives the main rotor shaft and the tail rotor shaft.

## 5.4 Main rotor thrust and tail rotor thrust

The equation (3.14) could be used to calculate the power coefficient of the main rotor, that is  $C_w \cong 0.006968$ , and the thrust coefficient  $C_u \cong 0.045965$ . It is also possible to find the maximum thrust  $u_{m,\max}$  that could be generated from the main rotor using the equation (3.12), setting the throttle at 100% and the collective angle at its maximum. The obtained result is

$$u_{m,\max} \cong 52729 \frac{\text{kg}\cdot\text{m}\cdot\text{rad}^2}{\text{s}^2}, \quad (5.3)$$

where  $\Omega_{m,\max} \cong 41.364303$  rad/sec,  $\alpha_{c,\max} = 0.541052$  rad,  $\rho = 1.225$  kg/m<sup>3</sup> are respectively the maximum angular speed, the maximum collective angle and the air density at 15 Celsius degrees and 1 atm, from Table 5.1.

In the same way, it is possible to find out the power coefficient and the thrust coefficient for the tail rotor which are respectively  $C_w^T \cong 0.100974$  and  $C_u^T \cong 0.273201$ . The maximum thrust which can be generated from the tail rotor is  $u_{t,\max} \cong 2601$  kg · m · rad<sup>2</sup>/s<sup>2</sup>, whose value is calculated using the throttle at 100%, the angular velocity  $\Omega_{t,\max} \cong 375.315601$  rad/sec and the maximum collective angle for the tail rotor  $\alpha_{c,\max}^T = 0.596903$  rad, from Table 5.1.

## 5.5 Drag term and friction terms

According to equation (3.16), the value of the drag term is  $\gamma \cong 0.154546$  m. Where, the middle value of the interval of the tail rotor collective angle is  $\alpha_{c,\text{mid}}^T \cong 0.151844$  rad, and the collective angle of the main rotor consistent with hovering is  $\alpha_{c,\text{hover}} \cong 0.268693$  rad, from equation (3.57).

The value of  $\ddot{p}$  in the equation (3.52) stands for acceleration. A positive component along the  $x$ -axis means an increase in velocity along that axis. Suppose to collect the tip velocity in each axis in the vector  $\dot{p}_{\max}$ . Given the maximum velocity of the helicopter, we know that, once reached that particular value, the acceleration of the helicopter along that axis will drop to 0, since the existence of a friction force in the opposed direction. This behaviour can be described as:

$$0 = R(\varphi_m + \varphi_t) - M_{\mathcal{H}}\bar{g}e_z - B\dot{p}_{\max}. \quad (5.4)$$

Looking closely to  $R(\varphi_m + \varphi_t)$ , namely the propelling force of the helicopter, it is easy to figure out that its form has to be special when the tip speed is reached, in fact:

- To reach the tip speed in  $z$ -axis it is necessary that the  $z$ -axis of the inertial reference frame  $\mathcal{F}_E$  and the body-fixed reference  $\mathcal{F}_B$  coincide.
- To reach the tip speed in  $x$ -axis we consider a motion at maximum speed due to a total thrust directed along the  $x$ -axis while in a horizontal attitude ( $R = I_3$ ). In this case, the thrust takes its maximum value (compatibly with the need to keep the helicopter hovering).

The Figure 5.3 shows the force components present in some particular helicopter attitudes. In the frame on the left the helicopter is horizontal, namely  $R = I_3$ , and all the forces belong to  $z$ -axis, disregarding forces exerted by the tail rotor. In the frame on the right the helicopter is in hovering condition, therefore the friction force  $F_z^3 = 0$ , while the friction force  $F_x^2$  along the  $x$ -axis is maximum.

The friction terms are calculated finding the tip speed of the helicopter and, for the EC135 P2+, the values are summarized in Table 5.4. Since we only know the maximum linear speed along the  $x$ -axis, we consider as null the friction force along the  $y$ -axis.

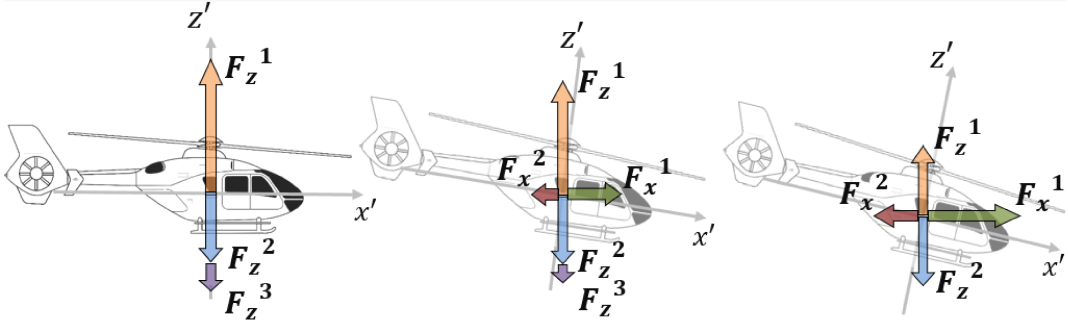


Figure 5.3: Friction terms increasing horizontal speed. The variables are defined as

$$F_z^1 = e_z^\top \varphi, F_z^2 = M_{\mathcal{H}} \bar{g}, F_z^3 = e_z^\top \dot{p} \beta_v, F_x^1 = e_x^\top \varphi, F_x^2 = e_x^\top \dot{p} \beta_h.$$

|                  | Limit values |           |              | Condition  |
|------------------|--------------|-----------|--------------|--|
|                  | [m/s]        | [rad/sec] | min – max[%] |  |
| Airspeed         | 79.7         |           |              | sea level,<br>+20 Celsius degrees,<br>gross mass up to 2300,<br>TOP mode |
| Rate of climbing | 8.9          |           |              |  |
| Hover turning    |              | 1.047     |              |  |
| Throttle range   |              |           | 97 - 104     |  |

Table 5.4: Airspeed value ([8] page 23). Hover turning velocity and throttle range (page 43 and 35 in [3]). Rate of climbing (page 60 in [9]).

Using the equation (5.4) and the speed limit values, it is possible to calculate  $\beta_h$  and  $\beta_v$ , respectively the friction term along  $x$ -axis and  $z$ -axis. In order to do that, we fill the vector which contains the maximum speed as  $\dot{p}_{\max} = [79.7 \ 8.9]^\top$ , referring to the Table 5.4. Then we should consider the results from (3.59) and therefore set  $\alpha_r = 0$  and  $\alpha_p = \arccos\left(\frac{2 M_{\mathcal{H}} \bar{g}}{u_{m,\max}}\right) \cong 1.014333$  rad. We end up with an equation depending on the term  $\beta_h$ , where the other terms are known:

$$2\beta_h e_x^\top \dot{p}_{\max} = u_{m,\max} \sin\left(\arccos\left(\frac{2 M_{\mathcal{H}} \bar{g}}{u_{m,\max}}\right)\right), \quad (5.5)$$

where  $e_x = [1 \ 0 \ 0]^\top$ . The equation (5.5) would allow to find the value of the friction term, however the pitch angle  $\alpha_p = \arccos\left(\frac{2 M_{\mathcal{H}} \bar{g}}{u_{m,\max}}\right) := \bar{\alpha}_p$  is not reachable because of the structure constraints of the swash-plate. In fact,  $\bar{\alpha}_p$  does not belong to the range showed in the Table 5.1. However, the thrust vector sought could be performed from the helicopter. In fact, the thrust vector direction could not only be managed with the *cyclic control* angles, namely  $\alpha_p$  and  $\alpha_r$ , but also with the helicopter's attitude. For instance, fixing the helicopter's attitude, we can still change the main rotor attitude using the swash-plate which could be thought of as a spherical joint with some structure limits. For example, a solution in which the pitch angle belongs to the structural limits range is the one with the *cyclic control* angles fixed to zero and the fuselage tilted along the  $z$ -axis with respect to  $y$ -axis in the earth-fixed reference frame  $\mathcal{F}_E$  at the pitch value angle found  $\bar{\alpha}_p$ . Consider that the hover condition is preserved, and that in this particular solution we do not involve rolling and pitching terms.

The friction term  $\beta_v$  can be found fixing  $\alpha_p = 0$ ,  $\alpha_r = 0$  and  $R = \text{diag}(1, 1, 1)$ , which are the conditions to reach the maximum velocity along the  $z$ -axis. From the equation (5.4), we thus obtain

$$\beta_v e_z^\top \dot{p}_{\max} = \frac{1}{2} u_{m,\max} - M_{\mathcal{H}} \bar{g}. \quad (5.6)$$

Instantiating equations (5.5) and (5.6) with known values, the friction coefficients can be easily computed. It has been found that  $\beta_h \cong 281 \text{ kg}\cdot\text{s}^{-1}$  and  $\beta_v \cong 1398 \text{ kg}\cdot\text{s}^{-1}$ .

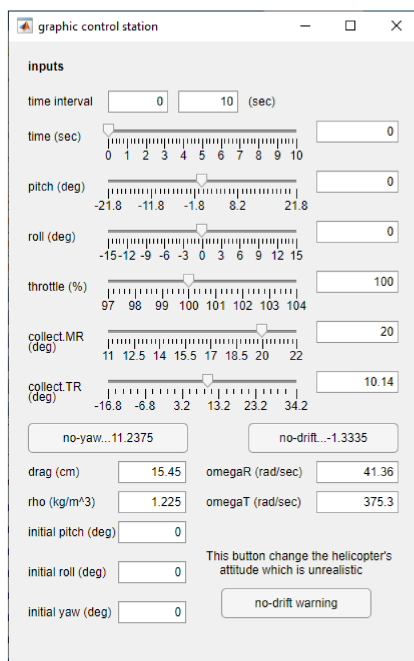
Using the same method, it is possible to estimate the value of  $\beta_r$ , the friction term linked to the yaw velocity. Let us assume the helicopter in hovering condition, with  $\dot{\xi}_m = \dot{\xi}_t = 0$ . At the maximum yaw speed (along  $z$ -axis) the angular acceleration will be null. Since we consider a hovering condition with  $\alpha_r = \alpha_p = 0$ , the total torque  $\tau$  is equal to  $\frac{1}{2}(D_t u_{t,\max} - \gamma u_{m,\text{hover}}) \xi_z$ . Therefore, from equation (4.6) we get  $0 = S^{-1} \left( [\hat{J}_{\mathcal{H}}^*, \xi_{\max}^2] + (D_t u_{t,\max} - 2\gamma M_{\mathcal{H}} \bar{g} - \beta_r \langle \xi_{\max}, \xi_z \rangle) \xi_z \right) S^{-1}$ , where  $\xi_{\max}$  denotes the maximal yawing speed that, from the Table 5.4, is known to be  $\xi_{\max} = 1.047 \cdot \xi_z$  (rad/sec). Thus, isolating the friction term, this equation becomes:

$$\beta_r \langle \xi_{\max}, \xi_z \rangle \xi_z = [\hat{J}_{\mathcal{H}}^*, \xi_{\max}^2] + (D_t u_{t,\max} - 2\gamma M_{\mathcal{H}} \bar{g}) \xi_z. \quad (5.7)$$

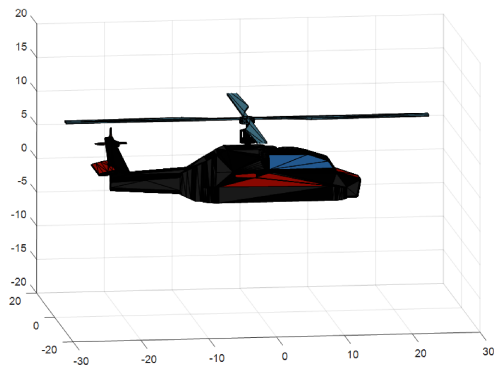
To find out the correct value of the friction term it is necessary to fill the equation (5.7), namely the tip thrust of the tail rotor  $u_{t,\max}$ , the structural values, and the drag coefficient found. The result for this parameter is  $\beta_r \cong 10797 \text{ N}\cdot\text{m}\cdot\text{s}\cdot\text{rad}^{-1}$ .

## Numerical experiments and results

A series of tests of the mathematical model have been carried out using MATLAB. In order to clarify what can be tested, and how, it could be useful to introduce the graphic control panel shown in Figure 6.1.



(a) Graphic interface used to test the model.



(b) A graphic windows concerned to show the initial attitude of the helicopter, which is linked to the value of  $R$  selected.

Figure 6.1: Graphic input interface.

The cell *time interval* allows to set the time range for new experiments. The interface gives the possibility to perform series of test, therefore the initial value of *time interval* could not be set at an instant of time  $t_1$  until another experiment, which ended at  $t_1$ , has been completed. The slider named *Time* shows the selected instant of time in a pop-up animation window. Every slider is linked to an editable cell, hence, any value belonging to the correct range could be directly written. The five sliders *pitch*, *roll*, *throttle*, *collect.MR*,



*collect.TR* are the interface to manage the value of the variables  $\alpha_p, \alpha_r, \Omega_m, \alpha_c, \alpha_c^T$ . The *no-yaw* button sets the angle  $\alpha_c^T$  for no yawing condition, from equation (3.60), whereas the button *no-drift* manages the value of  $\alpha_r$  to achieve no-drifting condition using the equation (3.61). The two editable cells *drag* and *rho* interacts respectively with the values of the variables  $\gamma$  and  $\rho$ . The three cells *initial roll*, *initial pitch*, *initial yaw* interface with the matrix  $R$  forcing a value of attitude of the helicopter along the three axes  $x, y, z$ . The button *no-drift warning* changes the *initial roll* value in order to achieve a stationary no drifting condition, technique introduced in the third test.

**First test - lift response:** The first test made lasts 10 seconds and it does not involve pitch and roll angles ( $\alpha_p = 0, \alpha_r = 0$ ), moreover the throttle is set at 100% and the tail rotor collective angle at  $\alpha_{c,\text{mid}}^T$ . About the main rotor collective angle, it has been chosen in order to produce lift along  $z$ -axis. The value chosen is 20 degrees. Figure 6.2 shows the result of the computation. By the analysis of the first test we can see that the position along  $x$ -axis is pretty constant, which could seem reasonable because pitch angle is not involved. In the other hand, there is a clear decrease of  $p$  along  $y$ -axis due to drift effect, take into account that the direction of the tail rotor thrust is opposite to  $y$ -axis, as Figure 3.1 shows. The  $z$  component of  $\tau$  is negative, and this is the cause of clockwise yawing. Looking closely to the position  $p$ , along the  $x$ -axis it can be observed a little decrease due to the combined action of the helicopter yawing and tail rotor drift. In fact, when the helicopter nose turns, the drift effect causes a slight decrease along the  $x$ -axis. Note that the drift force exerted by the tail rotor is the  $y$  component of  $\varphi$ , which is  $e_y^T \varphi$ . The last remarkable thing which could be seen from the first test is that the  $z$  component of  $\varphi$  has the value of 16191 N, which is more than the helicopter-weight force, that could be determined from Table 5.2 as  $1420 \cdot \bar{g} \cong 13925$  N. The result force along the  $z$ -axis is positive and as described by the graph of the  $z$  component of  $p$  the helicopter lifts up.

*Remark:* The referring  $x, y$  and  $z$  variables in the  $\tau$  graphic have been extract from the equation (3.2) following the construction of  $\tau$ . In the specific, these variables are  $e_z^T \tau e_y$ ,  $e_x^T \tau e_z$ , and  $e_y^T \tau e_x$ .

**Second test - no yaw:** The next example lasts 5 seconds and illustrates how to select the tail rotor collective angle using the equation (3.60) to achieve no yaw condition. From the graph of  $\tau$  it is clear that the torque exerted on the helicopter becomes null. Consequently, the slight decrease of the position along the  $x$ -axis, which was a side effect of the yawing, is no more present. The result is presented in Figure 6.4

**Third test - neither yaw nor drift:** The third test is introduced as a simplification to delete the drift effect. In this case the  $y$  component of  $p$  is not decreasing anymore, since the helicopter's attitude has been changed using the *no-drift warning* button in the control graphic panel. This does not cause a change in the angle of attack of the blades as before, but in the *initial roll* angle and, as a consequence, in the matrix  $R$ . In fact, the helicopter's attitude is rotated at the angle determined by the equation (3.61) along the  $x$ -axis, and the rotation causes an equilibrium among the drift effect and the thrust along the  $y$ -axis. The equilibrium among the forces causes a constant value of  $p$  along the  $y$ -axis

as wanted.  $M_\theta$  is the matrix used to compute the rotation, whose form is

$$M_\theta = \begin{bmatrix} 1 & 0 & 0 \\ 0 & \sin \theta & -\sin \theta \\ 0 & \sin \theta & \sin \theta \end{bmatrix}.$$

The new initial value of the the Lie group matrix used is  $\bar{R} = R \cdot M_\theta$ . The result of the experiment is shown in Figure 6.4. It is interesting to figure out that the  $\varphi$  components does not change, since it is described in the body reference frame  $\mathcal{F}_B$ . Indeed, changing the attitude of the helicopter does not concern  $\mathcal{F}_B$ , but the relation of the two reference systems  $\mathcal{F}_B$  and  $\mathcal{F}_E$ .

**Fourth test - pitch response:** From now on new tests will be computed starting from the result of the third test. Therefore, the first 3 seconds will be common to every execution. The fourth test is about pitch response. The pitch angle of attack has been set at 5 degrees constant starting from the third second to the end. In the result, illustrated in Figure 6.5, it can be seen an increase of the  $y$  component of  $\tau$ . It is also possible to notice, as Figure 5.3 shows, that the change in the angle of attack causes a variation in the  $\varphi$  components. Indeed, the  $x$  component of  $\varphi$ , that is  $e_x^\top \varphi = \frac{1}{2} u_m \sin \alpha_p \cos \alpha_r$ , increases as  $\alpha_p$  increases, whereas the  $z$  component of  $\varphi$ , that is  $e_z^\top \varphi = \frac{1}{2} u_m \cos \alpha_p \cos \alpha_r$ , decreases as the  $\alpha_p$  increases.

**Fifth test - positive roll response:** In this test we set the angle  $\alpha_r$  from the third second to the sixth second at 5 degrees. The result is presented in Figure 6.6 and shows an increase of the  $x$  component of  $\tau$ . This behaviour follows the equation (3.54), where  $\alpha_r$  is linked to the  $x$  component of  $\tau$ . In addition, using the same equation it is immediate to see that the  $y$  component of  $\tau$  is zero because  $\alpha_p = 0$ . Remark that instead the  $z$  component of  $\tau$  is zero because of the no-yaw condition. As the previous example, a change of the angle of attack causes the  $z$  component of  $\varphi$  to decrease, moreover the magnitude of the  $y$  component of  $\varphi$  increases because of the changing in the thrust caused by positive rolling and the tail rotor drift effect have an according direction. It is important to point out, in the graph of  $p$ , that the rolling of the helicopter causes a falling situation, because of the thrust reduction. In the other hand, the helicopter position along the  $y$ -axis decreases drastically.

**Sixth test - Main rotor collective response:** The *collective control* is amply used for managing the acceleration of the helicopter. The test of this specific control system has been made increasing up to 22 degrees the main rotor collective angle starting from the third second to the tenth second. The increase of the main rotor collective angle causes a thrust boost which increases the lifting of the helicopter. The result is shown in Figure 6.7. As remarked, every time *collective control* is changed the helicopter driver has to adjust also the tail rotor collective angle, since the no-yaw flight mode depends on  $u_m$ , which is a function of  $\alpha_c$ . This could be seen in the  $z$  component of  $\tau$  whose magnitude changes and needs to be managed through the *pedals control*.

**Seventh test - negative roll response:** The Figure 6.8 shows results of a test in which it has been tried to remove the drift effect using the *cyclic control*. It has already been

remarked that a force control is not sufficient to remove the drift effect, since a combined helicopter's attitude control is needed. The no-drift flight mode could be achieved, for example, using a PID control on the helicopter's attitude. This test was carried out using as initial setting the same setting as for the second test, whereas the last 7 seconds are computed using the equation (3.61) to change  $\alpha_r$ . It is important to notice that the equation used would ensure the no-drift situation, but because of the absence of PID controller the helicopter rolling is not stopped at all. Therefore the helicopter ends up in a non controllable rolling condition, which determines loss of control.

***Eight test - free flight:*** The eighth test consist in a simulation of a free flight with multiple inputs for the *cyclic control* and the *collective control*. The result is shown in Figure 6.9, moreover Table 6.1 presents the time line of the controls used. The *throttle* during the test is constant to 100%.

| Eighth test          |              |         |         |         |         |          |
|----------------------|--------------|---------|---------|---------|---------|----------|
| <i>time interval</i> | <i>(sec)</i> | [0 - 2[ | [2 - 4[ | [4 - 6[ | [6 - 8[ | [8 - 10] |
| $\alpha_p$           | <i>(deg)</i> | 0       | 0.5     | -0.5    | -0.3    | 0        |
| $\alpha_r$           | <i>(deg)</i> | 0       | 0       | 0       | 0.8     | -2       |
| $\alpha_c$           | <i>(deg)</i> | 20      | 22      | 22      | 22      | 20       |
| $\alpha_c^T$         | <i>(deg)</i> | 11.24   | 11.24   | 8.5     | 12.32   | 12.32    |

Table 6.1: Eighth test - free flight. The orange-colored numbers indicate that the *no-yaw* flight mode has been activated for that time window.

6. Numerical experiments and results

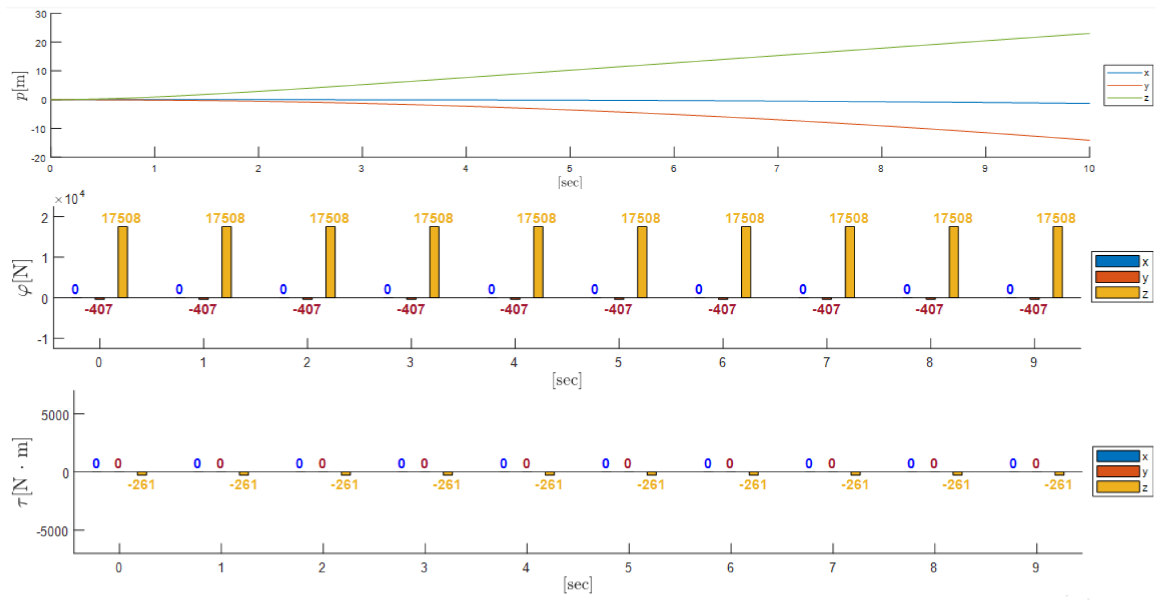


Figure 6.2: First test - lift response. Top panel: components of the position of  $c_H$ . Middle panel: components of the thrust. Bottom panel: components of the active torque generated by rotors.

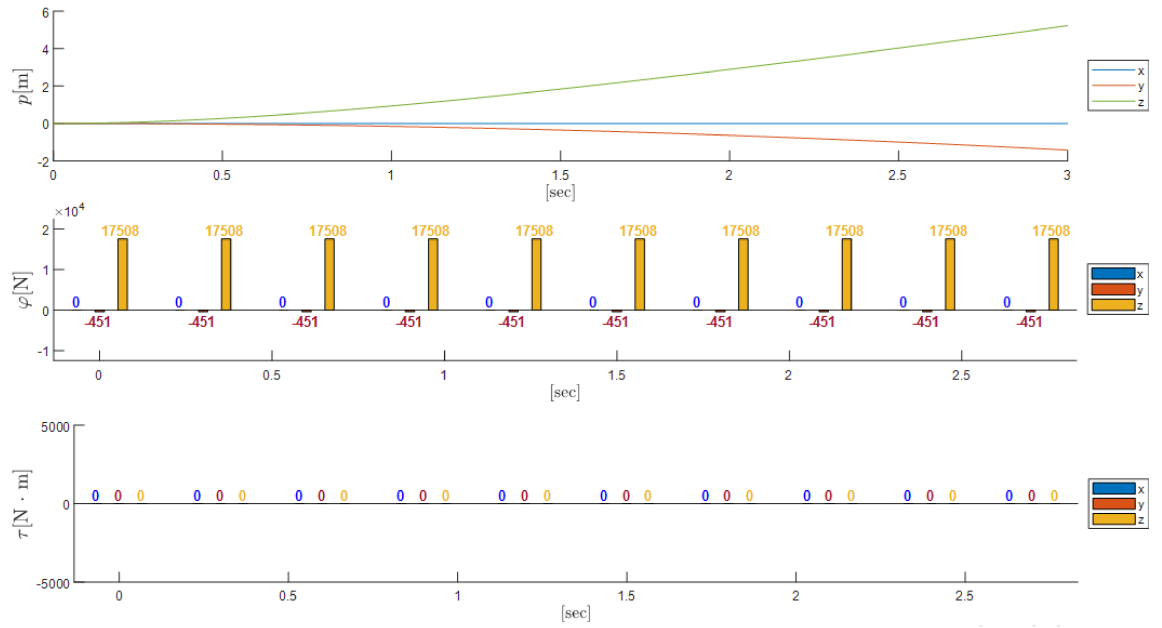


Figure 6.3: Second test - no yaw.

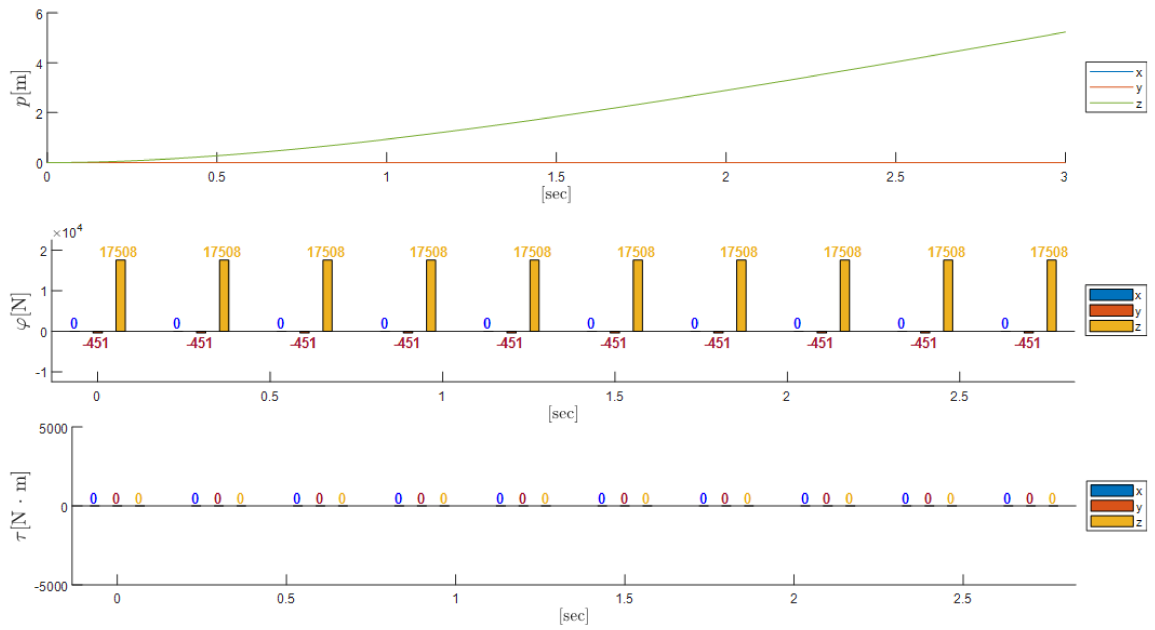


Figure 6.4: Third test - neither yaw nor drift.

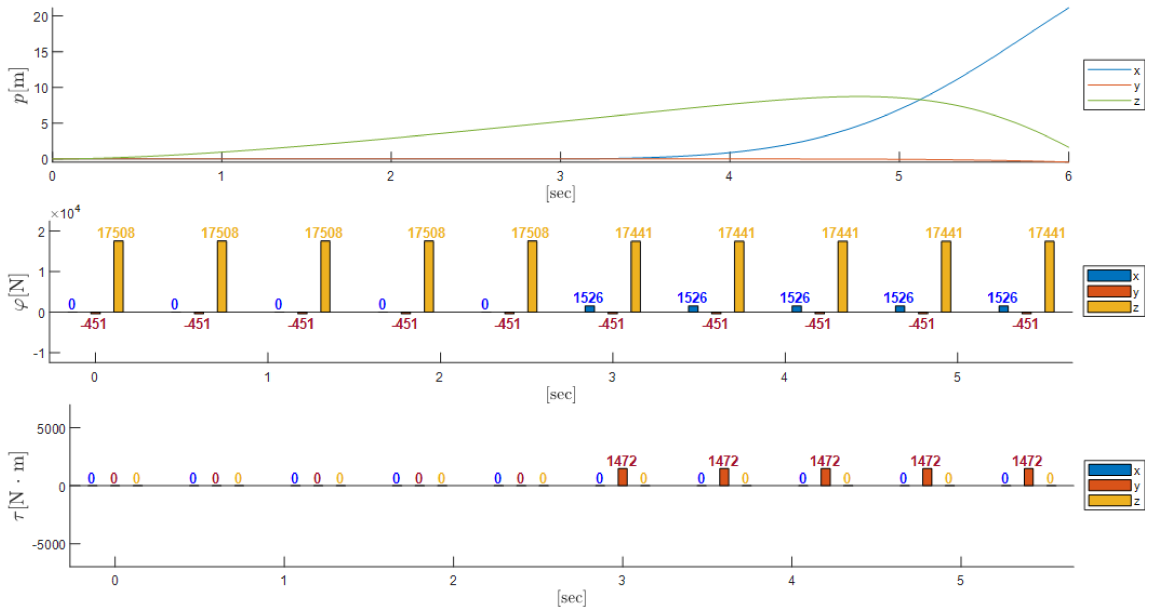


Figure 6.5: Fourth test - pitch response.

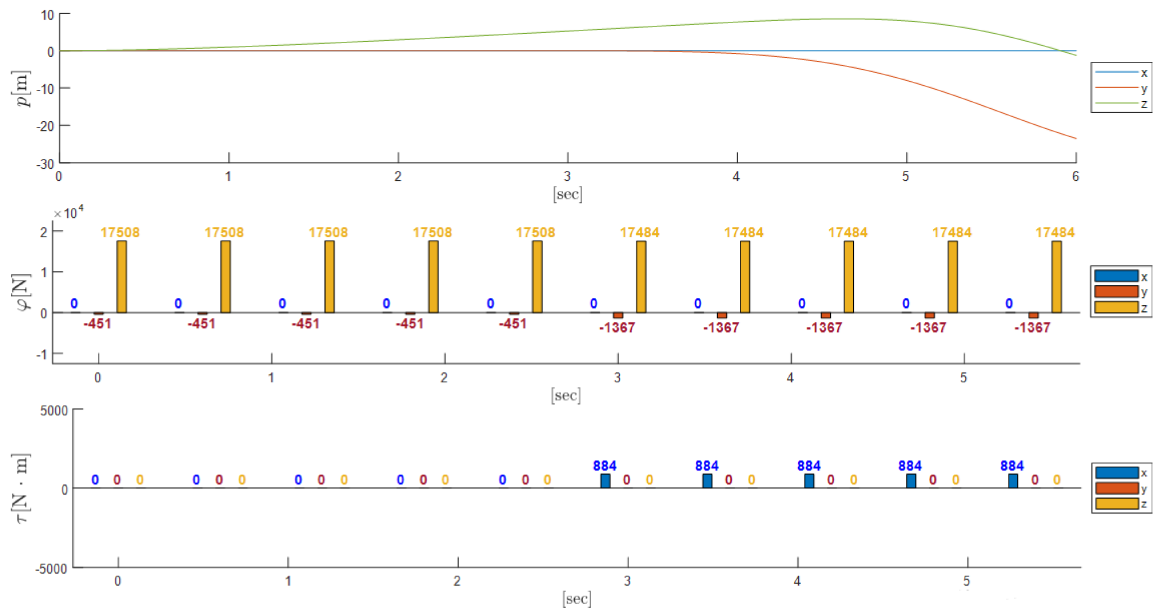


Figure 6.6: Fifth test - positive roll response.

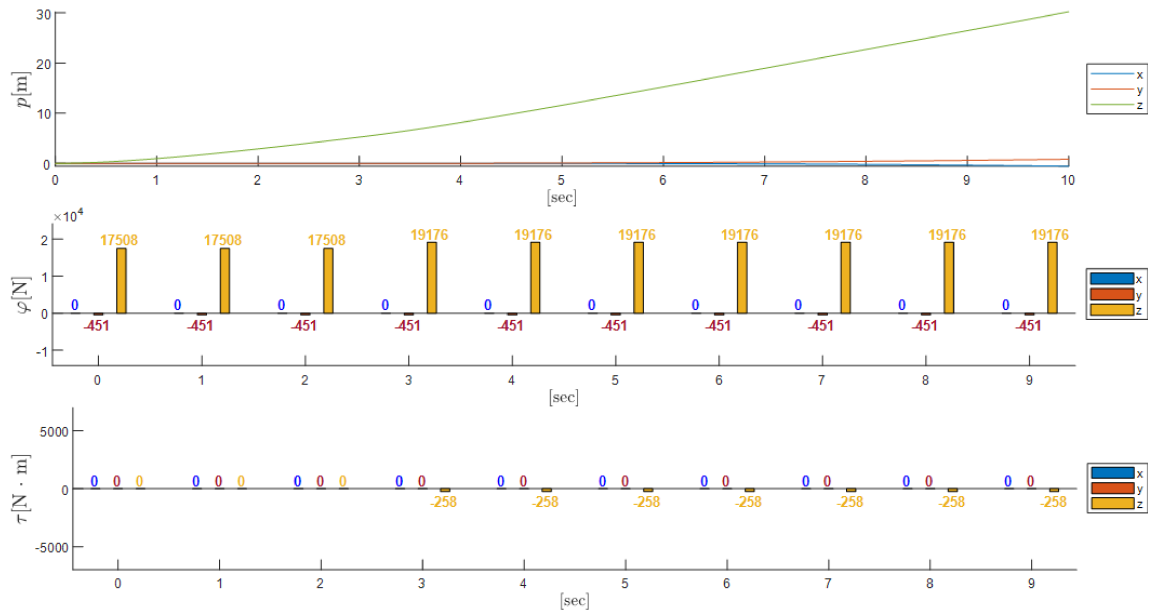


Figure 6.7: Sixth test - Main rotor collective response.

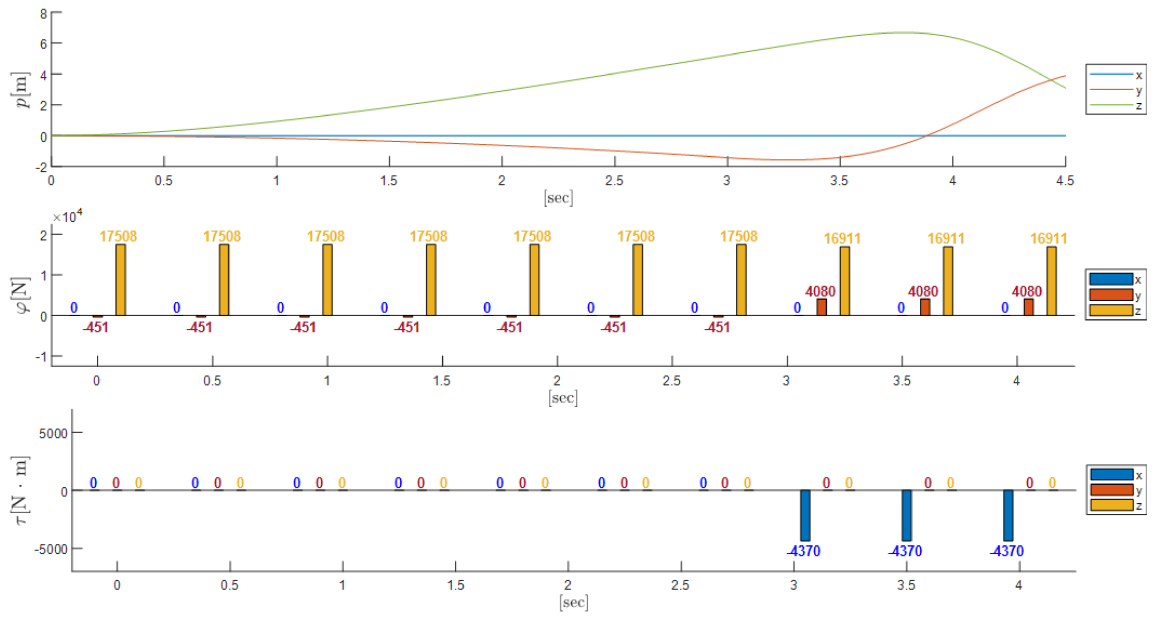


Figure 6.8: Seventh test - negative roll response.

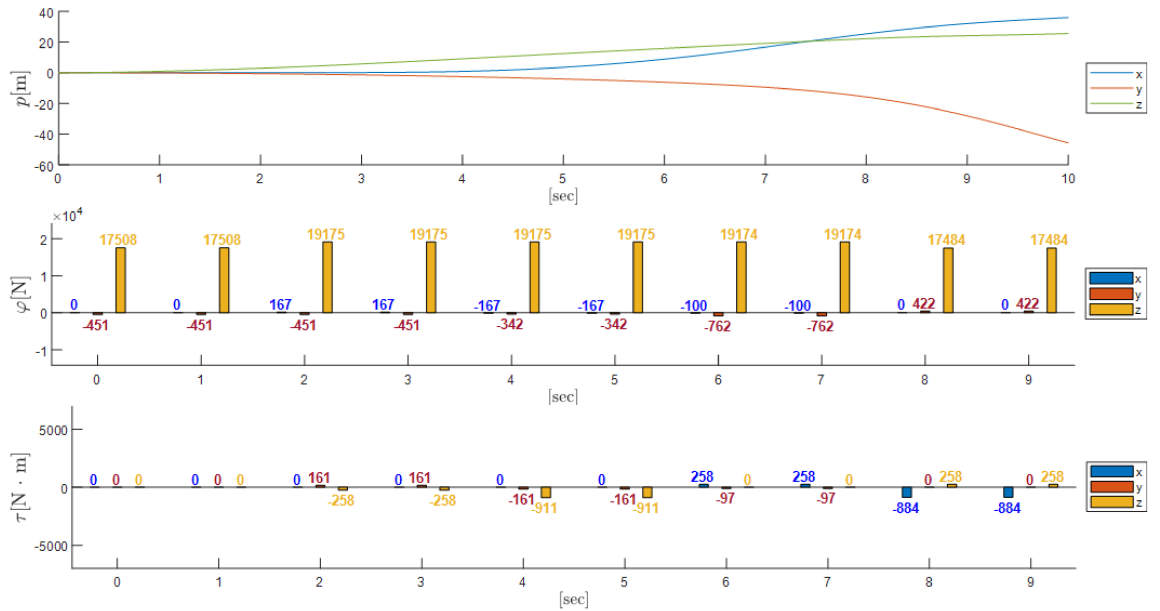


Figure 6.9: Eighth test - free flight.

---

## Conclusions

In this paper we discuss a mathematical model of a helicopter, which has been analysed and tested several times. The research continues with a comparison between the model found and other studies with the same focus in order to validate the model itself. The comparison has led to accept the resulting system of equations. Furthermore, we discuss about actuators, control systems and mechanical structures in order to define an interface to interact properly with the helicopter. During the implementation, we selected a commercial model of a helicopter to provide all the values required. This allowed the numerical implementation in MATLAB enhanced with graphical windows for graphs and flight simulations. Among all these pages we use mathematical formulations and test results to describe behaviours typical of a helicopter. In my opinion, this research will bring a new perspective on how to work with helicopters, and that perspective could help to easily implement control algorithms, such as Proportional Integral Derivative control and Virtual Attractive Repulsive Potentials control.



---

# Acknowledgements

This research has been performed during an internship at Tokyo University of Agriculture and Technology (TUAT) in Japan during the period between January and March 2020. The internship experience has taken place thanks to professor Toshihisa Tanaka who kindly allowed me to work and use the laboratory of signal and image processing in TUAT Koganei Campus. Finally, I would like to thank my supervisor, professor Simone Fiori, for the passion he shared and the support he provided me during the research and also during my entire experience abroad.

---

# Bibliography

- [1] EUROCOPTER DEUTSCHLAND GmbH, Helicopter Training Center, P.O. Box 1353, D-86603, Donauwörth (Germany), *EC 135 – Training Manual*, 7 2002.
- [2] M. Kobilarov, M. Desbrun, J. Marsden, and G. Sukhatme, “A discrete geometric optimal control framework for systems with symmetries,” in *Robotics: Science and Systems*, (Atlanta, GA, USA), pp. 161 – 168, June 2007.
- [3] EUROCOPTER DEUTSCHLAND GmbH, Helicopter Training Center, P.O. Box 1353, D-86603, Donauwörth (Germany), *Flight Manual EC135 P2+*, 2002.
- [4] *The EC135 Drive Train Analysis and Improvement of the Fatigue Strength*, September 2007.
- [5] K. Kampa, B. Enenkl, G. Polz, and G. Roth, “Aeromechanical aspects in the design of the EC135,” in *23rd European Rotorcraft Forum in Dresden, Germany*, pp. 38.1–38.14, 1997.
- [6] Eurocopter, *Eurocopter training service, main rotor*, May 2006.
- [7] EASA European Aviation Safety Agency, *Type Certificate Data Sheet NO. IM.E.017 for PW206 & PW207 series engines*.
- [8] EASA European Aviation Safety Agency, *Type Certificate Data Sheet No. EASA.R.009 for EC135*.
- [9] EUROCOPTER DEUTSCHLAND GmbH, Helicopter Training Center, P.O. Box 1353, D-86603, Donauwörth (Germany), *Eurocopter EC135 technical data*, 2006.
- [10] S. Kim and D. Tilbury, “Mathematical modeling and experimental identification of an unmanned helicopter robot with flybar dynamics,” *Journal of Robotic Systems*, vol. 21, no. 3, pp. 95 – 116, 2004.
- [11] T. Salazar, “Mathematical model and simulation for a helicopter with tail rotor,” in *Advances in Computational Intelligence, Man-Machine Systems and Cybernetics*, pp. 27 – 33, World Scientific and Engineering Academy and Society, 2010.

- [12] P. Talbot, B. Tinling, W. Decker, and R. Chen, “A mathematical model of a single main rotor helicopter for piloted simulation,” tech. rep., NASA, September 1982.
- [13] R. Abraham, J. Marsden, and T. Ratiu, *Manifolds, Tensor Analysis, and Applications*. Springer, 1988.
- [14] F. Bullo and A. Lewis, *Geometric Control of Mechanical Systems: Modeling, Analysis, and Design for Mechanical Control Systems*. Springer, 2005.
- [15] S. Fiori, “Nonlinear damped oscillators on Riemannian manifolds: Fundamentals,” *Journal of Systems Science and Complexity*, vol. 29, no. 1, pp. 22 – 40, 2016.
- [16] S. Fiori, “Nonlinear damped oscillators on Riemannian manifolds: Numerical simulation,” *Communications in Nonlinear Science and Numerical Simulation*, vol. 47, pp. 207 – 222, 2017.
- [17] A. Bloch, P. Krishnaprasad, J. Marsden, and T. Ratiu, “The Euler-Poincaré equations and double bracket dissipation,” *Communications in Mathematical Physics*, vol. 175, pp. 1 – 42, 1996.
- [18] Z.-M. Ge and T.-N. Lin, “Chaos, chaos control and synchronization of a gyrostat system,” *Journal of Sound and Vibration*, vol. 251, no. 3, pp. 519 – 542, 2002.
- [19] S. Fiori, “Model formulation over Lie groups and numerical methods to simulate the motion of gyrostats and quadrotors,” *Mathematics*, vol. 7, no. 10, 2019.
- [20] C. Rotaru and M. Todorov, “Helicopter flight physics,” in *Flight Physics – Models, Techniques and Technologies* (K. Volkov, ed.), IntechOpen, 2018.
- [21] W. Yu and Z. Pan, “Dynamical equations of multibody systems on Lie groups,” *Advances in Mechanical Engineering*, vol. 7, no. 3, pp. 1 – 9, 2015.
- [22] B. E. Axelsson, J. C. Fulmer, and J. P. Labrie, *Design of a Helicopter Hover Test Stand*. Bachelor Science Thesis in Aerospace Engineering, Worcester Polytechnic Institute (Worcester, MA, USA), March 2015.